Kinetics and Mechanism of Nucleophilic Substitutions on Coordinated Polyenes and Polyenyls. 3.[1] Activation of η^5-Cyclopentadienyl Ligands toward Nucleophilic Attack through $\eta^5 \rightarrow \eta^3$ Ring Slippage and a Comparison with Reaction at C_5H_4O in $[Ru(\eta^5\text{-}C_5H_5)(\eta^4\text{-}C_5H_4O)(L)]^+$ (L = CH_3CN, Pyridine, Thiourea)

Walter Simanko,[†] Walter Tesch,[†] Valentin N. Sapunov,[†] Kurt Mereiter,[‡] Roland Schmid,[†] and Karl Kirchner*[,†,§]

Institute of Inorganic Chemistry and Institute of Mineralogy, Crystallography, and Structural Chemistry, Technical University of Vienna, Getreidemarkt 9, A-1060 Vienna, Austria

John Coddington and Scot Wherland*[,||]

Department of Chemistry, Washington State University, Pullman, Washington 99164-4630

Received August 17, 1998

Complexes of the types $[Ru(\eta^5\text{-}C_5H_5)(\eta^4\text{-}C_5H_4O)]_2(CF_3SO_3)_2$ (**1**) and $[Ru(\eta^5\text{-}C_5H_5)(\eta^4\text{-}C_5H_4O)(L)]CF_3SO_3$ (L = CH_3CN (**2**), pyridine (**3**), thiourea (**4**)) react with tertiary phosphines to give (i) 1,1′- (**12**) or (ii) 1,2-disubstituted ruthenocenes (**13**) depending primarily on the basicity of the entering phosphine and the nature of L. Path i proceeds via the intermediacy of $[Ru(\eta^3\text{-}C_5H_5)(\eta^4\text{-}C_5H_4O)(PR_3)]_2^{2+}$ (**5**) and $[Ru(\eta^3\text{-}C_5H_5)(\eta^4\text{-}C_5H_4O)(PR_3)(L)]^+$ (**6**−**8**); i.e., the hapticity of the C_5H_5 ligand is changed from η^5 to η^3 while forming an additional Ru−P bond. The η^3 bonding mode was established by ^1H and $^{13}C\{^1H\}$ NMR spectroscopies. The kinetics of these reactions were studied in detail, providing enthalpies and entropies of both activation and reaction. The conversions to **6**−**8** are exothermic ($\Delta H° = -5.5$ to -16.9 kcal mol^{-1}) but entropically unfavorable ($\Delta S° = -44.8$ to -19.0 cal K^{-1} mol^{-1}). The activation parameters and rate constants vary little with the phosphine, suggesting a preequilibrium between η^5 and η^3 species of the starting complexes where the latter reacts with the entering phosphine in the rate-determining step. The new η^3-C_5H_5 complexes are, with the exception of **5**, fluxional in solution due to an intramolecular enantiomeric equilibrium likely proceeding through a five-coordinate η^1-C_5H_5 intermediate. Path ii proceeds via η^3-cyclopentenoyl complexes of the type $[Ru(\eta^5\text{-}C_5H_5)(\eta^3\text{-}C_5H_4O\text{-}2\text{-}PR_3)(L)]^+$ (**9**−**11**). Furthermore, **3** and **4** react with small and basic phosphines $PR_3 = PMe_3$ and $Me_2PCH_2PMe_2$ to give the half-sandwich complexes $[Ru(\eta^5\text{-}C_5H_4OH)(PR_3)_2L]^+$ (**14**, **15**) together with free $C_5H_4PR_3$ (**16**).

Introduction

Nucleophilic attack at metal-coordinated ligands constitutes one of the most useful procedures in synthetic organic chemistry for obtaining new regio- and stereoselectively functionalized molecules. Such processes are particularly facile if the metal center is coordinatively saturated, substitutionally inert, and sufficiently electron-deficient. For the ligands, nonconjugated and conjugated olefins are among the most reactive substrates, while aromatic ligands, in particular the cyclopentadienyl anion, are among the least reactive.[2] It was thus a surprise to find that tertiary phosphines react with the cationic 18-electron complexes $[Ru(\eta^5\text{-}C_5H_5)(\eta^4\text{-}C_5H_4O)]_2^{2+}$ (**1**) and $[Ru(\eta^5\text{-}C_5H_5)(\eta^4\text{-}C_5H_4O)(L)]^+$ (L = CH_3CN (**2**), pyridine (**3**), thiourea (**4**)) to give 1,1′-disubstituted ruthenocenes $[Ru(\eta^5\text{-}C_5H_4PR_3)(\eta^5\text{-}C_5H_4OH)]^+$ (**12**) (paths i and ii, Scheme 1) as well as the anticipated 1,2-disubstituted ruthenocenes (**13**), formed via η^3-cyclopentenoyl complexes $[Ru(\eta^5\text{-}C_5H_5)(\eta^3\text{-}C_5H_4O\text{−}PR_3)(L)]^+$ (path iii, Scheme 1).[1,3] Scheme 1 gives an overview of the reactions hitherto analyzed on a synthetic level. Thus, **1** yields only **12** irrespective of the nature of the phosphine, whereas complexes **2**−**4** give **13** as well. Preliminary kinetic studies with PMe_3 as the nucleophile have shown[1] that the formation of **12** is far more complex than that of **13**. In the initial step, PMe_3 attacks the metal center to give the η^3-C_5H_5 intermediate [Ru-

[†] Institute of Inorganic Chemistry.
[‡] Institute of Mineralogy, Crystallography, and Structural Chemistry.
[§] E-mail: kkirch@mail.zserv.tuwien.ac.at.
[||] E-mail: scot_wherland@wsu.edu.

(1) Part 2: Simanko, W.; Sapunov, V. N.; Schmid, R.; Kirchner, K.; Wherland, S. *Organometallics* **1998**, *17*, 2391.
(2) Davies, S. G.; Green, M. L. H.; Mingos, D. M. P. *Tetrahedron* **1978**, *34*, 3047.
(3) (a) Kirchner, K.; Taube, H. *J. Am. Chem. Soc.* **1991**, *113*, 7039. (b) Kirchner, K.; Mereiter, K.; Schmid, R.; Taube, H. *Inorg. Chem.* **1993**, *32*, 5553. (c) Kirchner, K.; Mereiter, K.; Mauthner, K.; Schmid, R. *Inorg. Chim. Acta* **1994**, *217*, 203. (d) Simanko, W.; Vallant, T.; Mereiter, K.; Schmid, R.; Kirchner, K.; Coddington, J.; Wherland, S. *Inorg. Chem.* **1996**, *35*, 5923.

10.1021/om980701t CCC: $15.00
Publication on Web 12/01/1998

Scheme 1

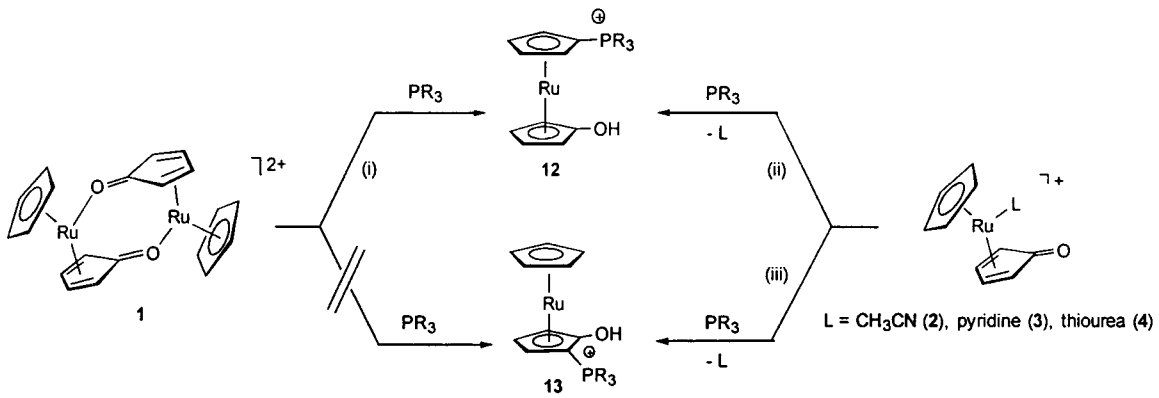

PR_3 = (i) **1**; $P\{(2,4,6\text{-}OMe)_3C_6H_2\}_3$, PCy_3, PMe_3, PBu^n_3, PMe_2Ph, $PMePh_2$, PPh_3

(ii) **2**; PCy_3, PMe_3, PPr^n_3, PBu^n_3, PMe_2Ph

3; PMe_3

4; PMe_3

(iii) **2**; $P\{(2,4,6\text{-}OMe)_3C_6H_2\}_3$, $PMePh_2$, $P(p\text{-}PhOMe)_3$, PPh_3

3; PCy_3, PMe_3, PBu^n_3, PMe_2Ph, $PMePh_2$

4; PCy_3, PMe_3, PBu^n_3, PMe_2Ph

Scheme 2

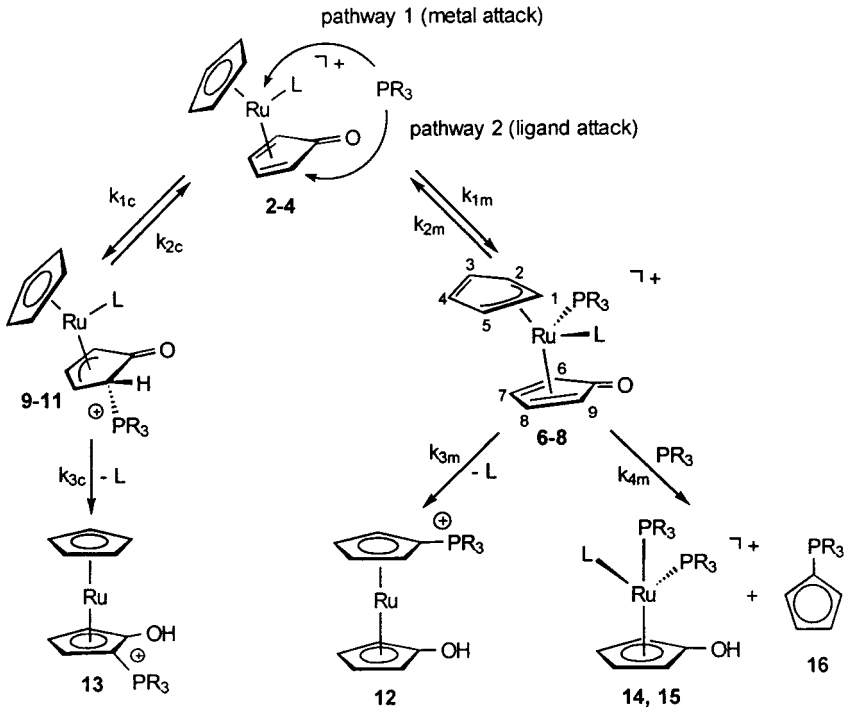

$(\eta^3\text{-}C_5H_5)(\eta^4\text{-}C_5H_4O)(PMe_3)(L)]^+$ which then undergoes an endo migration of PMe_3 to give $[Ru(\eta^5\text{-}C_5H_4PMe_3)(\eta^5\text{-}C_5H_4OH)]^+$ (**12a**) and/or free $C_5H_4PMe_3$ together with the half-sandwich complex $[Ru(\eta^5\text{-}C_5H_4OH)(PMe_3)_2L]^+$ (**14a**, **15**), depending on L (Schemes 1 and 2).[1,3]

The process of η^5 to η^3 ring slippage of $\eta^5\text{-}C_5H_5$ ligands (possibly also η^3 to η^1 ring slippage) is an appealing way of activating C_5H_5 systems toward nucleophilic attack. The occurrence of η^3 intermediates appears to be of more general importance. Such species have been postulated frequently as a mechanistic rationale for a number of stoichiometric[4] and catalytic[5] organometallic reactions. These include α- and β-hydrogen abstractions,[6,7] photochemically induced C−H, Si−H, and C−C bond cleavages,[8] cyclopentadienyl ligand transfers,[9] and ligand

(4) (a) Yan, X.; Cherenga, A. N.; Metzler, N.; Green, M. L. H. *J. Chem. Soc., Dalton Trans.* **1997**, 2091. (b) Green, J. C.; Parkin, R. P. G.; Yan, X.; Haaland, A.; Scherer, W.; Tafipolsky, M. A. *J. Chem. Soc., Dalton, Trans.* **1997**, 3219. (c) Butts, M. D.; Bergman, R. G. *Organometallics* **1994**, *13*, 1899.

(5) Sigman, M. S.; Fatland, A. W.; Eaton, B. E. *J. Am. Chem. Soc.* **1998**, *120*, 5130.

substitutions.[10] Unfortunately, the few reports dealing with additions, substitutions, and migrations of nucleophiles onto the C_5H_5 ligand do not allow definite conclusions to be drawn regarding the involvement of ring slippage.[11] Herein we report the kinetics and mechanism of nucleophilic addition and substitution reactions of tertiary phosphines with **1**−**4**. In particular, we present kinetic and thermodynamic data for the formation of the 1,1′-disubstituted products via reversible formation of η^3-C_5H_5 intermediates (Scheme 2). In addition, the facile and reversible η^5 to η^3 transformations to the novel η^3-C_5H_5 complexes $[Ru(\eta^3\text{-}C_5H_5)(\eta^4\text{-}C_5H_4O)(PR_3)]_2^{2+}$ (**5**) and $[Ru(\eta^3\text{-}C_5H_5)(\eta^4\text{-}C_5H_4O)(PR_3)(L)]^+$ (**6**−**8**) have been studied by low-temperature NMR spectroscopy. Our mechanistic investigations are supported by extended Hückel molecular orbital calculations. Further data on the reactions that lead to the 1,2-disubstituted ruthenocenes are presented, and the origin of the selectivity between the two ruthenocene products is discussed.

Results and Discussion

Syntheses and Spectroscopic Studies. We have previously shown that the dimeric complex $[Ru(\eta^5\text{-}C_5H_5)(\eta^4\text{-}C_5H_4O)]_2(CF_3SO_3)_2$ (**1**) reacts with tertiary phosphines to give exclusively 1,1′-disubstituted ruthenocenes **12** in essentially quantitative yield (Scheme 1).[3] To detect and identify intermediates, this reaction with the tertiary phosphines PMe_3, PCy_3, $P\{(2,4,6\text{-}OMe)_3C_6H_2\}_3$, and PPh_3 has been monitored by NMR spectroscopy. These phosphines have been chosen since they cover a large range of nucleophilicity and size. The nucleophilicity is taken to increase in the order of increasing pK_a[12] PPh_3 (2.73) < PMe_3 (8.65) < PCy_3 (9.70) < $P\{(2,4,6\text{-}OMe)_3C_6H_2\}_3$ (11.02), while the bulkiness of the phosphines, as expressed by their cone angles,[13] increases in the order PMe_3 (118°) < PPh_3 (145°) < PCy_3 (170°) < $P\{(2,4,6\text{-}OMe)_3C_6H_2\}_3$ (184°). Below −70 °C, the dimeric complexes $[Ru(\eta^3\text{-}C_5H_5)(\eta^4\text{-}C_5H_4O)(PR_3)]_2^{2+}$ (**5a**−**c**) are formed quantitatively (Scheme 3), except for the weakly nucleophilic PPh_3, for which about 70% unreacted **1** was observed at equilibrium. Upon an increase in the temperature above −70 °C, all of these complexes are cleanly converted to complexes **12a**,**e**,**f**,**g** with no other intermediates detectable. The identity of **5a**−**d** has been unequivocally established by ^{1}H and ^{31}P-{^{1}H} NMR spectroscopies and in the case of **5a** also by ^{13}C{^{1}H} NMR spectroscopy. The ^{1}H NMR spectra of **5a**−**d** are consistent with both the ketonic oxygen of the C_5H_4O moiety and the phosphine attached at the metal center; i.e., the complex is both dimeric and chiral. Complexes **5** are not fluxional (vide infra), and consequently, in the ^{1}H NMR spectrum the protons of the C_5H_5 and C_5H_4O ligands give rise to nine individual resonances. The ^{13}C{^{1}H} NMR spectrum of **5a** exhibits altogether 10 individual resonances for the C_5H_5 and C_5H_4O ligands. The resonance of the "ketonic" carbonyl carbon at 166.3 ppm is high-field shifted with respect to the corresponding resonance in **1** (cf. 183.3 ppm in **1**), indicating that the C_5H_4O ligand has become somewhat more electron rich (partially reduced). Note that, for the final products **12**, where the η^4-bound cyclopentadienone ligand is already fully reduced to an η^5-bound hydroxycyclopentadienyl system, the resonance of the C−O carbon atom is found in the range 127−129 ppm.

Scheme 3

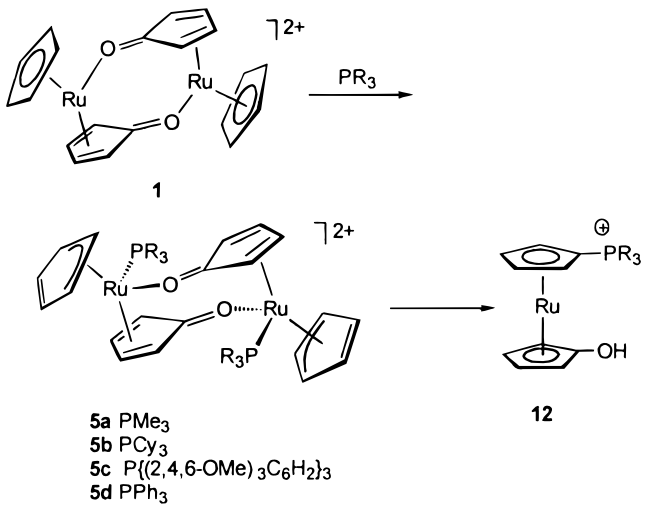

Surprisingly, the dimeric nature of **5** is maintained even if **1** is treated with the strongly basic bidentate ligand $Me_2PCH_2PMe_2$. Instead of the expected monomeric complex $[Ru(\eta^3\text{-}C_5H_5)(\eta^4\text{-}C_5H_4O)(\eta^2(P,P)\text{-}Me_2PCH_2PMe_2)]CF_3SO_3$, the dimeric complex $[Ru(\eta^3\text{-}C_5H_5)(\eta^4\text{-}C_5H_4O)(\eta^1(P)\text{-}Me_2PCH_2PMe_2)]_2(CF_3SO_3)_2$ (**5e**) is obtained with the $Me_2PCH_2PMe_2$ ligand coordinated in η^1(P)-fashion (cf. Scheme 4). Due to the η^1(P) coordination mode of the $Me_2PCH_2PMe_2$ ligand, in the ^{31}P{^{1}H} NMR spectrum the resonance of the coordinated PMe_2 group is significantly downfield shifted with respect to the noncoordinated PMe_2 moiety, giving rise to a doublet

(6) (a) Marks, T. J.; Kolb, J. R. *J. Am. Chem. Soc.* **1975**, *97*, 3397. (b) Brintzinger, H. H.; Bercaw, J. E. *J. Am. Chem. Soc.* **1970**, *92*, 3397. (c) Slocum, D. W.; Beach, D. L.; Ernst, C. R.; Fellows, R.; Moronski, M.; Conway, B.; Bencini, J.; Siegel, A. *J. Chem. Soc., Chem. Commun.* **1980**, 1043. (d) Roman, E.; Astruc, D.; Des Abbayes, H. *J. Organomet. Chem.* **1981**, *219*, 211. (e) Slocum, D. W.; Engelmann, T. R.; Fellows, R. L.; Moronski, M. Duraj, S. *J. Organomet. Chem.* **1984**, *260*, C21. (f) Slocum, D. W.; Moronski, M.; Gooding, R.; Duraj, S. *J. Organomet. Chem.* **1984**, *260*, C26.

(7) Yang, G. K.; Bergman, R. G. *Organometallics* **1985**, *4*, 129.

(8) (a) Green, M. L. H.; Berry, M.; Couldwell, C.; Prout, K. *Nouv. J. Chim.* **1977**, 1950. (b) Berry, M.; Elmitt, K.; Green, M. L. H. *J. Chem. Soc., Dalton Trans.* **1979**, 1950. (c) Ephritikhine, M.; Green, M. L. H. *J. Chem. Soc., Chem. Commun.* **1976**, 926. (d) Rest, A. J.; Whitwell, I.; Graham, W. A. G.; Hoyano, J. K.; McMaster, A. D. *J. Chem. Soc., Chem. Commun.* **1984**, 624. (e) Yang, H.; Kotz, K. T.; Asplund, M. C.; Harris, C. B. *J. Am. Chem. Soc.* **1997**, *119*, 9564.

(9) (a) Peng, M. H.; Brubaker, C. H., Jr. *J. Organomet. Chem.* **1977**, *135*, 333. (b) Lee, J. G.-S.; Brubaker, C. H., Jr. *Inorg. Chim. Acta* **1977**, *25*, 181.

(10) (a) Vest, P.; Anhaus, J.; Bajaj, H. C.; van Eldik, R. *Organometallics* **1991**, *10*, 818. (b) Rerek, M. E.; Basolo, F. *J. Am. Chem. Soc.* **1984**, *106*, 5908. (c) Cramer, R.; Seiwell, L. P. *J. Organomet. Chem.* **1975**, *92*, 245.

(11) (a) Arif, A. M.; Cowley, A. H.; Nunn, C. M.; Pakulski, M. *J. Chem. Soc., Chem. Commun.* **1987**, 994. (b) Benfield, F. W. S.; Green, M. L. H. *J. Chem. Soc., Dalton Trans.* **1974**, 1324. (c) Forschner, T. C.; Cooper, N. J. *J. Am. Chem. Soc.* **1989**, *111*, 7420. (d) McNally, J. M.; Cooper, N. J. *J. Am. Chem. Soc.* **1989**, *111*, 4500. (e) Hughes, R. P.; Maddock; S. M.; Rheingold, A. L.; Liable-Sands, L. M. *J. Am. Chem. Soc.* **1997**, *119*, 5988. (f) Herber, U.; Bleuel, E.; Gevert, O.; Laubender, M.; Werner, H. *Organometallics* **1998**, *17*, 10. (g) de Azevedo, C. G.; Calhorda, M. J.; Carrondo, M. A. A. F. d. C. T.; Dias, A. R.; Duarte, M. T.; Galvão, A. M.; Gamelas, C. A.; Gonçalves, I. S.; da Piedade, F. M.; Romão, C. C. *J. Organomet. Chem.* **1997**, *544*, 257.

(12) (a) Golovin, M. N.; Rahman, Md. M.; Belemonte, J. E.; Giering, W. P. *Organometallics* **1985**, *4*, 1981. (b) Bush, R. C.; Angelici, R. J. *Inorg. Chem.* **1988**, *27*, 681. (c) Chenm, L.; Poë, A. J. *Coord. Chem. Rev.* **1995**, *143*, 265.

(13) Tolman, C. A. *Chem. Rev.* **1977**, *77*, 313.

Scheme 4

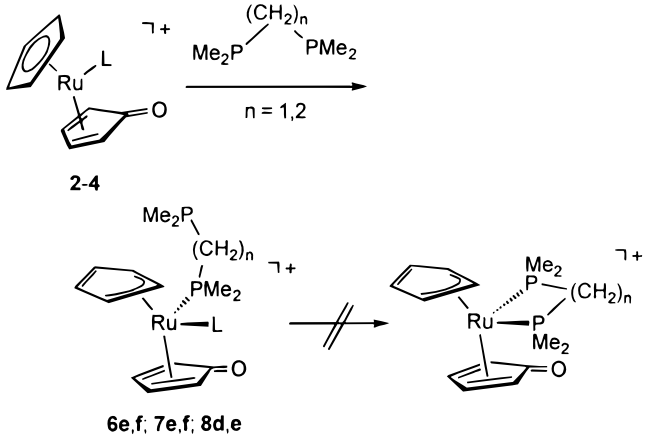

centered at 29.5 ppm ($^2J_{PP}$ = 35.9 Hz). The signal of the noncoordinated PMe_2 moiety exhibits a doublet centered at −43.4 ppm ($^2J_{PP}$ = 35.9 Hz).

The monomeric complex [Ru(η^5-C_5H_5)(η^4-C_5H_4O)(CH_3CN)]CF_3SO_3 (**2**) reacts with PR_3 (PMe_3, PBu^n_3, PMe_2Ph) in acetone at −90 °C to afford the complexes [Ru(η^3-C_5H_5)(η^4-C_5H_4O)(PR_3)(CH_3CN)]CF_3SO_3 (**6a**−**c**) in quantitative yield (Scheme 2). Upon an increase in the temperature, complexes **6a**−**c** are quantitatively converted to complexes **12a**−**c**. In the course of this reaction, no other intermediates could be detected. The reaction of **2** with $PMePh_2$ is less selective, as revealed by ^{1}H NMR spectroscopy. At −90 °C, two competing reactions take place to give the complexes [Ru(η^3-C_5H_5)(η^4-C_5H_4O)($PMePh_2$)(CH_3CN)]CF_3SO_3 (**6d**) and [Ru(η^5-C_5H_5)(η^3-C_5H_4O-$PMePh_2$)(CH_3CN)]CF_3SO_3 (**9a**) in a 1.3:1 ratio with complete consumption of **2**. At higher temperatures, **9a** and **6d** (**6d** via the intermediacy of **2** and **9a**) are cleanly converted to the 1,2-disubstituted ruthenocene [Ru(η^5-C_5H_5)(η^5-C_5H_3OH-2-$PMePh_2$)]CF_3SO_3 (**13d**) with no evidence found for the formation of the 1,1′-disubstituted ruthenocene [Ru(η^5-$C_5H_4PMePh_2$)(η^5-C_5H_4OH)]CF_3SO_3 (**12d**) (Scheme 2). It is noteworthy that, at low temperature, **2** does not react with PPh_3, while, at ambient temperature, [Ru(η^5-C_5H_5)(η^5-C_5H_3-OH-2-PPh_3)]CF_3SO_3 (**13e**) is exclusively formed. In the case of the bulky phosphine P{(2,4,6-OMe)$_3C_6H_2$}$_3$, no evidence for the formation of an η^3-C_5H_5 complex is found even at −90 °C, and the 1,2-disubstituted ruthenocene [Ru(η^5-C_5H_5)(η^5-C_5H_3OH-2-P{(2,4,6-OMe)$_3$-C_6H_2}$_3$)]CF_3SO_3 (**13g**) is formed exclusively.

The ^{1}H and ^{13}C{^{1}H} NMR spectra of **6** are consistent with binding of the cyclopentadienyl ligand in an η^3-fashion. In the ^{1}H NMR spectra of **6**, the olefinic hydrogens $H^{3,4}$ absorb at about 5.6 ppm, the terminal allylic hydrogen atoms $H^{2,5}$ absorb at about 3.8 ppm, and the central allyl hydrogen H^1 absorbs at about 4.4 ppm. Complexes **6** are chiral. In contrast to **5**, complex **6** is fluxional in solution, and thus, the η^3-C_5H_5 ligand exhibits only three proton and carbon resonances (in a 2:1:2 ratio) and the C_5H_4O ring shows only two hydrogen and three carbon resonances. This process is in the fast exchange region for 250 MHz ^{1}H NMR, even at −90 °C in acetone-d_6. Even though **6** is fluxional, the CH_3CN ligand is substitutionally inert (vide infra). Accordingly, the reaction of **2** with either $Me_2PCH_2PMe_2$ or $Me_2PCH_2CH_2PMe_2$ does not lead to the formation of [Ru(η^3-C_5H_5)(η^4-C_5H_4O)(η^2(P,P)-$Me_2PCH_2PMe_2$)]CF_3SO_3 and [Ru(η^3-C_5H_5)(η^4-C_5H_4O)(η^2(P,P)-$Me_2PCH_2CH_2PMe_2$)]CF_3SO_3, respectively, but instead gives [Ru(η^3-C_5H_5)(η^4-C_5H_4O)(η^1(P)-$Me_2PCH_2PMe_2$)(CH_3CN)]CF_3SO_3 (**6e**) and [Ru(η^3-C_5H_5)(η^4-C_5H_4O)(η^1(P)-$Me_2PCH_2CH_2PMe_2$)(CH_3CN)]CF_3SO_3 (**6f**) with the phosphine ligands bound in an η^1(P)-fashion (Scheme 4). Similarly to **2**, but at higher temperatures (≤−20 °C), [Ru(η^5-C_5H_5)(η^4-C_5H_4O)(py)]CF_3SO_3 (**3**) reacts with PR_3 (PMe_3, PBu^n_3, PMe_2Ph, or PCy_3) to yield quantitatively [Ru(η^3-C_5H_5)(η^4-C_5H_4O)(PR_3)(py)]CF_3SO_3 (**7a**−**d**) (Scheme 2). Complexes **7** are formed quantitatively even at room temperature but are unstable under this condition, being readily converted to complexes **13a**−**c** and **13f**.[3d] This reaction proceeds via the intermediacy of the η^3-cyclopentenoyl complexes [Ru(η^5-C_5H_5)(η^3-C_5H_4O-PR_3)(py)]CF_3SO_3 (**10**).[3] Complex **7a** reacts in a less selective way to give a mixture of **12a** and **13a**. With the phosphines $PMePh_2$ and PPh_3, no reaction takes place at low temperature. At ambient temperature, $PMePh_2$ reacts with **3** to yield quantitatively **13d**. This reaction proceeds via the η^3-cyclopentenoyl complex **10d**. The strongly basic chelating bis(phosphines) $Me_2PCH_2PMe_2$ and $Me_2PCH_2CH_2PMe_2$, on the other hand, react with **2** to give complexes of the type [Ru(η^3-C_5H_5)(η^4-C_5H_4O)(η^1(P)-$Me_2PCH_2PMe_2$)(py)]CF_3SO_3 (**7e**) and [Ru(η^3-C_5H_5)(η^4-C_5H_4O)(η^1(P)-$Me_2PCH_2CH_2PMe_2$)(py)]CF_3SO_3 (**7f**), respectively (Scheme 4).

Interestingly, in the presence of >2 equiv of PMe_3, an alternative mode of reaction, which again is highly selective, is observed. Complex **7a** is slowly converted to the half-sandwich complex [Ru(η^5-C_5H_4OH)(PMe_3)$_2$(py)]CF_3SO_3 (**14a**) and free $C_5H_4PMe_3$ (**16a**)[14] in essentially quantitative yield as monitored by ^{1}H, ^{13}C{^{1}H}, and ^{31}P{^{1}H} NMR spectroscopies. The same reaction occurs with $Me_2PCH_2PMe_2$, leading to the formation of [Ru(η^5-C_5H_4OH)(η^2(P,P)-$Me_2PCH_2PMe_2$)(py)]CF_3SO_3 (**14b**) and free $C_5H_4PMe_2CH_2PMe_2$ (**16b**). This pathway, however, was not observed even with PBu^n_3 and thus appears to be limited to phosphines with small cone angles.

Attempts to isolate **7** in pure form usually failed due to equilibria with other species. However, addition of PMe_3 to a solution of **3** in acetone afforded **7a** as a pale yellow solid in essentially quantitative yield due to its insolubility in this solvent. In the solid state, **7a** can be handled for a short period of time. The IR spectrum of **7a** exhibits a strong C═O stretching frequency at 1593 cm^{-1} (cf. 1682 cm^{-1} for **3**[15] and 1709 cm^{-1} for free C_5H_4O[16]) indicating loss of π-electron density from this group to the ring and metal and, thus, a substantial decrease in bond order. This observation suggests that in complexes containing the [Ru(η^3-C_5H_5)(η^4-C_5H_4O)]$^+$ moiety, there is a strong resonance interaction with the carbonyl group leading to the limiting structure **II**. Thus, the loss of aromaticity of the C_5H_5 ring as a result of the $\eta^5 \rightarrow \eta^3$ ring slippage process may be partially compensated for by the aromaticity gain of the C_5H_4O ring, a ground-state effect, although the crystal struc-

(14) Ladipo, F. T.; Anderson, G. K.; Rath, N. P. *Organometallics* **1994**, *13*, 4741.
(15) Kirchner, K.; Taube, H.; Scott, B.; Willett, R. D. *Inorg. Chem.* **1993**, *32*, 1430.
(16) Chapman, O. L.; McIntosh, C. L. *J. Chem. Soc., Chem. Commun.* **1971**, 770.

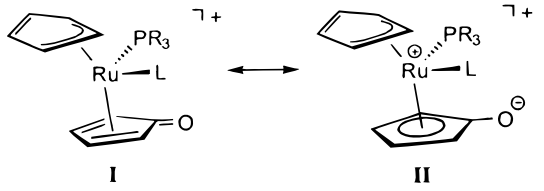

I **II**

tures of **1**−**4**[15] (Figures 1 and 2) show the C_5H_4O ring to be nonplanar and folded away from Ru by 13.7, 18.0, 18.8, and 18.9°, respectively. The identities of the intermediates **7** were established by ^1H, $^{13}C\{^1H\}$, and $^{31}P\{^1H\}$ NMR spectroscopies and in the case of **7a** also by elemental analysis. Complexes **7** are also fluxional in solution with the overall NMR spectroscopic features similar to those of **6** excepting the resonance of the hydrogen atom H^1. The latter experiences a shift of about −1.1 ppm relative to that of the analogous complexes **6** due to anisotropic shielding by the aromatic ring current of the pyridine placing the η^3-C_5H_5 ligand in an endo orientation (as drawn in the schemes). Only in this conformation is H^1 situated above the pyridine ring.

Likewise, $[Ru(\eta^5\text{-}C_5H_5)(\eta^4\text{-}C_5H_4O)(tu)]CF_3SO_3$ (**4**) is found to react with PMe_3, PBu^n_3, PMe_2Ph, $Me_2PCH_2PMe_2$, and $Me_2PCH_2CH_2PMe_2$ to yield the respective complexes $[Ru(\eta^3\text{-}C_5H_5)(\eta^4\text{-}C_5H_4O)(PR_3)(tu)]CF_3SO_3$ (**8a**−**e**) in quantitative yield as monitored by NMR spectroscopy (Scheme 2). In the case of $PMePh_2$ and PPh_3, no reaction takes place at low temperatures. When the temperature is raised, $PMePh_2$ is converted to the η^3-cyclopentenoyl complex **11d**. In the further course of reaction, however, **11d** decomposes to several intractable materials. The NMR spectra of complexes **8a**-**e** are similar to those of **6** and **7** and are not discussed here. It is interesting to note, however, that in contrast to the cases of **6** and **7**, when the temperature is lowered below about 0 °C, the signals of $H^{2,5}$, $H^{3,4}$, $H^{6,9}$, and $H^{7,8}$ broaden and eventually reemerge as eight distinct signals defining **8** as a chiral metal complex. The signal of the allylic proton H^1 remains unaffected by the exchange process, thus arguing against an exo/endo equilibrium. The same conclusion is drawn from $^{13}C\{^1H\}$ NMR spectroscopy. This has been demonstrated previously for **8a**.[1] The dynamic behavior of complexes **6**−**8** has been rationalized by an intramolecular enantiomeric equilibrium leading to an inversion of ruthenium as shown in Scheme 5. Site exchange by a dissociative process is excluded by the observation that the temperature dependence of the line shapes is unaffected by addition of thiourea or PMe_3. From the variable-temperature NMR studies, exchange rate constants were determined by visual comparison of the observed and computer-simulated spectra.[17] The rate constants derived from the different sets of coalescing resonances gave the same activation parameters. This points to the operation of a single exchange mechanism with $\Delta H^{\ddagger} = 12.3 \pm 0.4$ kcal mol^{-1} and $\Delta S^{\ddagger} = -0.3 \pm 1.3$ cal mol^{-1} K^{-1}. The rate constant (extrapolated to 298 K) of 5080 s^{-1} is about 2500 times greater than k_{2m} in Table 1, again signaling the absence of ligand dissociation in the enantiomeric conversion. Further support of this interpretation follows from the observations that the dimer **5** is not dynamic in nature and that in the intermediates of Scheme 4 the ligand L is nonlabile. An intramolecular isomerization process requires a vacant coordination site with appropriate orbital geometry which may be brought about by rearranging **6**−**8** toward a five-coordinate pseudo four-legged piano stool complex containing an η^1-C_5H_5 ligand (as drawn in Scheme 5) where the ligands L and PR_3 change their positions in a pseudorotational fashion.[18] For comparison, the activation enthalpies for such intramolecular ligand rear-

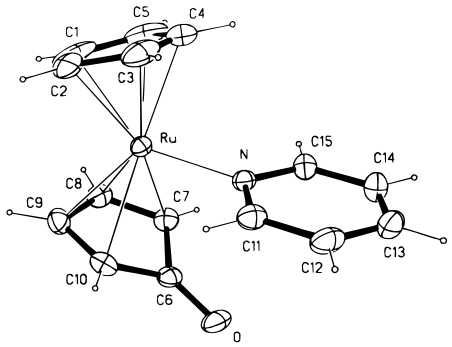

Figure 1. Structural view of $[Ru(\eta^5\text{-}C_5H_5)(\eta^4\text{-}C_5H_4O)(py)]CF_3SO_3$ (**3**) showing 20% thermal ellipsoids ($CF_3SO_3^-$ omitted for clarity). Selected bond lengths (Å): $Ru-C(1-5)_{av}$ 2.187(4), Ru−C(7) 2.240(3), Ru−C(8) 2.162(3), Ru−C(9) 2.159(3), Ru−C(10) 2.237(4), Ru−N 2.127(3), C(7)−C(8) 1.392(5), C(8)−C(9) 1.410(5), C(9)−C(10) 1.390(5), O(1)−C(6) 1.221(4).

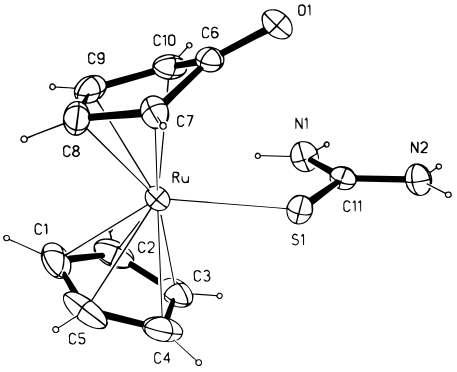

Figure 2. Structural view of $[Ru(\eta^5\text{-}C_5H_5)(\eta^4\text{-}C_5H_4O)(tu)]CF_3SO_3{\cdot}CH_3CN$ (**4**·CH_3CN) showing 20% thermal ellipsoids ($CF_3SO_3^-$ and CH_3CN omitted for clarity). Selected bond lengths (Å) and angle (deg): $Ru-C(1-5)_{av}$ 2.207(4), Ru−C(7) 2.259(2), Ru−C(8) 2.160(3), Ru−C(9) 2.151(3), Ru−C(10) 2.249(2), C(7)−C(8) 1.394(4), C(8)−C(9) 1.426(5), C(9)−C(10) 1.407(4), Ru−S(1) 2.399(1), O(1)−C(6) 1.229(3); Ru−S(1)−C(11) 110.6(1).

Scheme 5

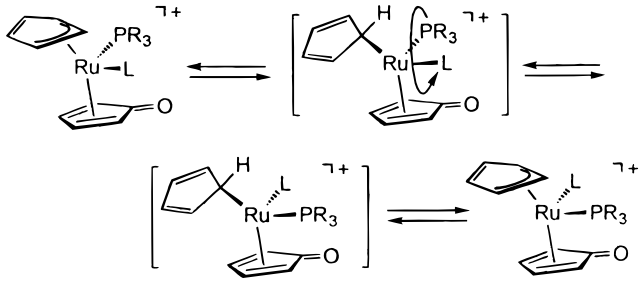

(17) (a) Binsch, G.; Kleier, D. *DNMR3, Program 165*; QCPE, Indiana University: Bloomington, IN, 1970. (b) Binsch, G.; Kessler, H. *Angew. Chem.* **1980**, *92*, 445.

(18) Galindo, A.; Mealli, C. *Inorg. Chem.* **1996**, *35*, 2406.

Table 1. Activation Parameter and Rate Constant Data at 25 °C for the Reactions of $[Ru(\eta^5\text{-}C_5H_5)(\eta^4\text{-}C_5H_4O)(L)]CF_3SO_3$ (L = CH_3CN (2), Pyridine (3), Thiourea (4)) with Tertiary Phosphines in Acetone To Give $[Ru(\eta^5\text{-}C_5H_4PR_3)(\eta^5\text{-}C_5H_4OH)]$ (12) via $[Ru(\eta^3\text{-}C_5H_5)(\eta^4\text{-}C_5H_4O)(PR_3)(L)]^+$ (6, 7, or 8)

PR_3 pK_a; cone angle, deg[c]	CH_3CN						pyridine			thiourea
	TTP[a] 11.0; 184	PMe_3[b] 8.65; 118	PPr^n_3 8.65; 131	PBu^n_3 8.43; 132	PMe_2Ph 6.50; 122	$PMePh_2$ 4.57; 136	PMe_3[b] 8.65; 118	PBu^n_3 8.43; 132	PMe_2Ph 6.50; 122	PMe_3[b] 8.65; 118
$\Delta H_{1m}^{\ddagger}$ [d]		4.9 ± 0.2	4.8 ± 0.1	5.7 ± 0.2	5.1 ± 0.4	8.5 ± 0.1	6.5 ± 0.2	6.3 ± 0.1	10.4 ± 0.3	7.5 ± 1.2
$\Delta S_{1m}^{\ddagger}$ [e]		−27.8 ± 0.6	−30.2 ± 0.4	−26.3 ± 0.5	−29.2 ± 1.4	−18.2 ± 0.4	−24.8 ± 0.7	−27.5 ± 0.4	−13.0 ± 1.2	−26.5 ± 4.0
k_{1m}, M^{-1} s^{-1}		1400	494	756	484	418	420	149	206	33
$\Delta H_{2m}^{\ddagger}$		20.1 ± 1.0	21.7 ± 1.8	19.6 ± 0.8	19.1 ± 0.8	14.0 ± 0.1	22.8 ± 1.2	17.0 ± 1.5	19.1 ± 0.3	20.2 ± 2.6
$\Delta S_{2m}^{\ddagger}$		9.8 ± 3.1	14.6 ± 5.9	9.9 ± 2.6	11.0 ± 2.7	0.9 ± 0.6	18.4 ± 3.7	4.4 ± 5.3	16.2 ± 1.1	10.8 ± 8.9
k_{2m}, s^{-1}		1.4	1.2	3.8	15.4	546	1.2	20	207	2
$\Delta H_m°$	−8.6 ± 0.3	−15.2	−16.9	−13.9	−14.0	−5.5	−16.3	−10.7	−8.7	−12.7
$\Delta S_m°$	−21.1 ± 1.1	−37.6	−44.8	−36.2	−40.2	−19.0	−43.2	−31.8	−29.2	−37.3
K_m, M^{-1}	53	1000	411	199	31	0.8	350	8	1	17
$\Delta H_{3m}^{\ddagger}$		20.8 ± 0.2	19.2 ± 0.1	21.1 ± 0.2	20.5 ± 0.4					
$\Delta S_{3m}^{\ddagger}$		12.6 ± 0.7	7.9 ± 0.4	15.3 ± 0.7	10.6 ± 1.4					
k_{3m}, s^{-1}		2.1	2.7	4.6	1.2	$<2 \times 10^{-2}$ [f]			$<10^{-3}$ [f]	

[a] TTP = P{(2,4,6-OMe)$_3$C$_6$H$_2$}$_3$. [b] Reference 1. [c] References 11 and 12. [d] All ΔH values in kcal mol^{-1}. [e] All ΔS values in cal mol^{-1} K^{-1}. [f] Estimated from product distribution.

rangements in the five-coordinate d^6 ruthenium complexes $Ru(PPh_3)_3Cl_2$ and $Ru(PPh_3)_3(H)(Cl)$ have been reported to be 10.0 ± 0.4 and 13.4 ± 0.6 kcal mol^{-1}, respectively.[19]

Finally, if PMe_3 is present in excess, **8a** reacts analogously to **7a** to give the half-sandwich complex $[Ru(\eta^5\text{-}C_5H_4OH)(PMe_3)_2(tu)]CF_3SO_3$ (**15**) together with free $C_5H_4PMe_3$ (**16a**) in quantitative yield as monitored by ^1H, $^{13}C\{^1H\}$, and $^{31}P\{^1H\}$ NMR spectroscopies (Scheme 2).

Cyclopentadienone is able to act, in addition to its simple diene function, both as a $2e^-$ oxidizing agent and as a one-proton acceptor while remaining coordinated. In this way it promotes the formation of substituted hydroxyruthenocenes in the final reaction step, i.e., the formation of complexes **12** and **13**. With respect to C_5H_5 ring activation, however, its role is less clear, and therefore, we prepared the cationic 1,3-butadiene complex $[Ru(\eta^5\text{-}C_5H_5)(\eta^4\text{-}C_4H_6)(CH_3CN)]CF_3SO_3$ (**17**) for comparison with the analogous cyclopentadienone complex **2**. Complex **17** has been prepared by the reaction of $[Ru(\eta^5\text{-}C_5H_5)(CH_3CN)_3]CF_3SO_3$ with 1,3-butadiene in moderate yield. Treatment of **17** with PMe_3 (>2 equiv) in acetone at room temperature gives the η^3-allyl complex $[Ru(\eta^5\text{-}C_5H_5)(\eta(1,2,3)\text{-}1\text{-}PMe_3\text{-}2\text{-buten-1-yl})(PMe_3)]PF_6$ (**18**) in 95% yield (Scheme 6). ^1H NMR monitoring indicated essentially quantitative conversion. However, with equimolar amounts of each reagent, the reaction is incomplete, but no complexes other than **17** and **18** together with free CH_3CN are observed. At lower temperatures, no reaction at all takes place, and there is no indication for the formation of an η^3-cyclopentadienyl complex. These observations suggest that the C_5H_4O ligand plays an important role in the ring slippage of C_5H_5. The formation of **18** involves regioselective addition of PMe_3 at the terminal carbon atom, as one would expect on the basis of the Davies−Green−Mingos rules.[2] Under these conditions, the addition is kinetically controlled, resulting in the sole formation of the anti η^3-allyl isomer (as drawn). However, the $\eta(1,2,3)$-4-PMe_3-2-buten-1-yl (anti CH_2PMe_3)

Scheme 6

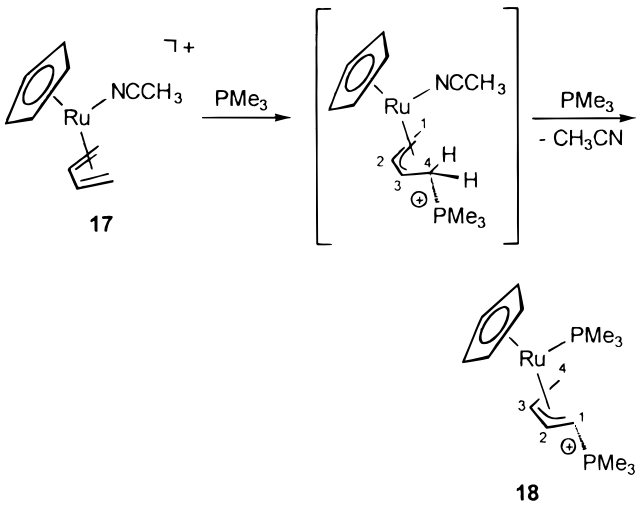

intermediate, which is not observed in the ^1H NMR spectrum, apparently undergoes a 1,4 hydrogen shift to give the more stable $\eta(1,2,3)$-1-PMe_3-2-buten-1-yl isomer **18** (anti Me, syn PMe_3 complex). In the course of this rearrangement, PMe_3 is also substituted for CH_3CN. A structural view of **18**, as determined by X-ray crystallography, is shown in Figure 3 with selected bond distances and angles given in the caption. The allyl moiety adopts an exo conformation with respect to the metal-coordinated PMe_3 ligand. This conformation is also maintained in solution, and no evidence for an endo/exo equilibrium is found. Complex **18** has been characterized by a combination of ^1H and ^{31}P NMR spectroscopies and elemental analysis.

Mechanistic Considerations. A mechanistic rationale for the transformation of the η^3-C_5H_5 intermediates **6**−**8** to the various products is given in Scheme 7. The activation of the already slipped C_5H_5 ligand in **6**−**8** may proceed via a further $\eta^3 \rightarrow \eta^1$ ring slippage process to give the coordinatively unsaturated species **A**. The presence of **A** is inferred from ^1H NMR spectroscopy. In an α-H elimination/H migration sequence (steps **A** → **B** → **C**) the 18-electron cyclopentadienylidene complex **C** is formed. It has to be noted that mononuclear complexes with a terminal cyclopentadienylidene ligand

(19) For intramolecular isomerizations of five-coordinate d^6 ruthenium complexes see: Hoffman, P. R.; Caulton, K. G. *J. Am. Chem. Soc.* **1975**, *97*, 4221. McNeil, K.; Anderson, K.; Bergman, R. G. *J. Am. Chem. Soc.* **1997**, *119*, 11244.

Scheme 7

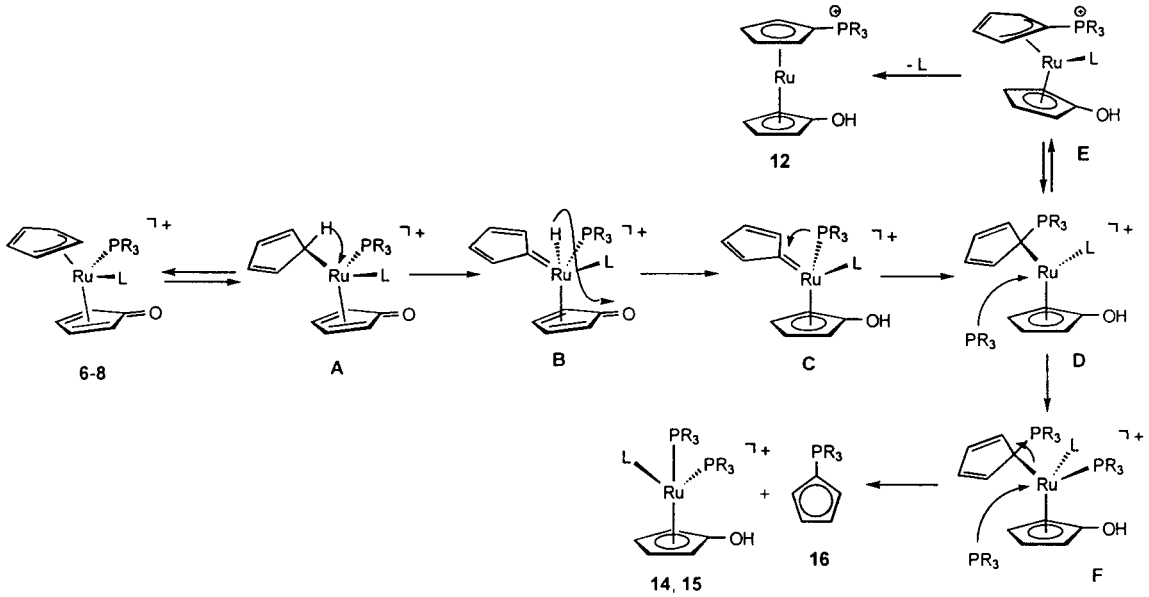

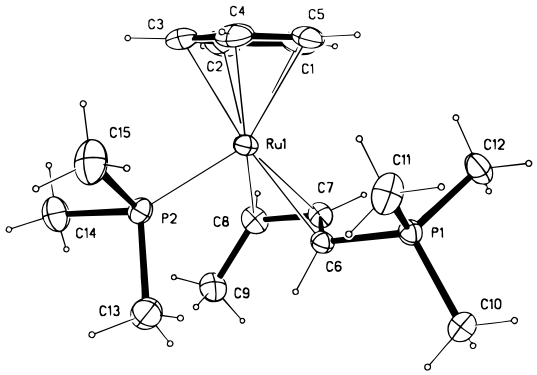

Figure 3. Structural view of $[Ru(\eta^5\text{-}C_5H_5)(\eta(1,2,3)\text{-}1\text{-}PMe_3\text{-}2\text{-buten-1-yl})(PMe_3)]PF_6$ (**18**) showing 20% thermal ellipsoids (only one of the two crystallographically independent complexes shown; PF_6^- omitted for clarity). Selected bond lengths (Å) and angle (deg): $Ru(1)-C(1-5)_{av}$ 2.207(5), Ru(1)−C(6) 2.187(4), Ru(1)−C(7) 2.101(4), Ru(1)−C(8) 2.220(4), Ru(1)−P(2) 2.304(1), C(6)−C(7) 1.431(5), C(7)−C(8) 1.430(6), C(8)−C(9) 1.505(6), C(6)−P(1) 1.767(4); C(6)−C(7)−C(8) 118.0(4).

are as yet unknown[20] but have been trapped by the formation of a [2+2] cycloaddition dimer[21] and have been postulated as intermediates in the decomposition of titanocene.[22] Subsequent migration of the coordinated phosphine to the α-carbon atom of the carbene moiety produces **D**. The latter, again a coordinatively unsaturated species, can generate the 1,1′-disubstituted product via **E** and release of L. This reaction is restricted to complexes with comparatively weak Ru−L bonds, viz. $Ru-(\mu)O{=}C_5H_4$ (**1**) and $Ru-NCCH_3$ (**2**). Alternatively, if phosphine is present in excess (>2 equiv) and attack of a second phosphine molecule at Ru intercepts the formation of **E**, due to a stronger Ru−L bond (L = pyridine, thiourea), intermediate **F** and eventually, via interaction of another PR_3 molecule, the half-sandwich complex $[Ru(\eta^5\text{-}C_5H_4OH)(PR_3)_2L]^+$ (**14**, **15**) together with free $C_5H_4PR_3$ (**16**) will be formed.

Kinetic Studies. The kinetic studies shown in Scheme 3 have been studied in detail by means of stopped-flow spectrophotometry and ^1H NMR spectroscopy, with the results summarized in Tables 1 and 2. The kinetic and NMR spectroscopic studies allow observation of two reaction pathways: reversible nucleophilic attack of PR_3 at the metal center providing the intermediate $[Ru(\eta^3\text{-}C_5H_5)(\eta^4\text{-}C_5H_4O)(L)(PR_3)]^+$ (**6**−**8**) (pathway 1) and reversible nucleophilic attack at the cyclopentadienone ligand giving an η^3-cyclopentenoyl complex $[Ru(\eta^5\text{-}C_5H_5)(\eta^3\text{-}C_5H_4O{-}PR_3)(L)]^+$ (**9**−**11**) (pathway 2).

The majority of the new kinetic results presented here involve attack of the nucleophile at Ru, leading to modification of the C_5H_5 ring and producing **12**. The details of the data collection and establishment of the rate laws are presented in the Experimental Section. A standard for comparison is the reaction of **2** with PPr^n_3. The data fit a two-term rate law involving reversible formation of an intermediate **6** followed by irreversible formation of the product **12**. The rate constants are identified in Scheme 3 as k_{1m} and k_{2m} for the first step and k_{3m} for the product formation step. An example of the data is presented in Figure 4. The data points are the high and low pseudo-first-order rate constants observed and the amplitude ratio, all at 25 °C. The solid lines represent the fit to all of the data (85 observations at 28 different conditions of temperature and PPr^n_3 concentration). The rate constants at 25 °C and their associated activation parameters for all reactions involving attack at Ru are presented in Table 1. The PPr^n_3 reaction is typical in showing a small activation enthalpy (4.8 kcal mol^{-1}) along with a large, negative entropy of activation (−30 cal mol^{-1} K^{-1}) for k_{1m}, characteristic of a bimolecular process. The two unimolecular processes, k_{2m} leading back to the reactants and k_{3m} leading to products, both have much larger activation enthalpies (21.7 and 19.2 kcal mol^{-1}, respectively) and positive activation entropies (15 and 8 cal mol^{-1} K^{-1}). The rest of the data in Table 1 were collected similarly, or with some variation when the apparent

(20) Wadepohl, H.; Galm, W.; Pritzkow, H.; Wolf, A. *Chem.—Eur. J.* **1996**, *2*, 1453.
(21) Hermann, W. A.; Plank, J.; Ziegler, M. L.; Weidenhammer, K. *Angew. Chem., Int. Ed. Engl.* **1978**, *17*, 777.
(22) Brintzinger, H. H.; Bercaw, J. *J. Am. Chem. Soc.* **1970**, *92*, 6182.

Table 2. Activation Parameter and Rate Constant Data at 25 °C for the Reactions of $[Ru(\eta^5\text{-}C_5H_5)(\eta^4\text{-}C_5H_4O)(L)]CF_3SO_3$ (L = CH_3CN (2), Pyridine (3), Thiourea (4)) with Tertiary Phosphines in Acetone To Give $[Ru(\eta^5\text{-}C_5H_5)(\eta^5\text{-}C_5H_4OH\text{-}2\text{-}PR_3)]$ (13) via $[Ru(\eta^5\text{-}C_5H_5)(\eta^3\text{-}C_5H_4O\text{-}2\text{-}PR_3)(L)]^+$ (9, 10, or 11)

PR_3 pK_a; cone angle, deg[c]	CH_3CN				pyridine			thiourea		
	TTP[a] 11.0; 184	$PMePh_2$[b] 4.57; 136	$P(PhOMe)_3$[b] 4.59; 145	PPh_3[b] 2.73; 145	TTP 11.0; 184	PMe_2Ph 6.50; 122	$PMePh_2$ 4.57; 136	TTP 11.0; 184	PMe_2Ph 6.50; 122	$PMePh_2$ 4.57; 136
$\Delta H_{1c}^{\ddagger}$ [d]	8.7 ± 0.2	13.1 ± 0.1	11.6 ± 0.1	11.6 ± 0.1	11.2 ± 0.2	14.8 ± 0.8	9.8 ± 0.5	10.3 ± 0.6	14.2 ± 0.1	15.9 ± 1.1
$\Delta S_{1c}^{\ddagger}$ [e]	−15.4 ± 0.7	−13.9 ± 0.5	−18.6 ± 0.2	−22.5 ± 0.5	−13.6 ± 0.7	−12.6 ± 2.5	−31.5 ± 1.6	−22.4 ± 2.0	−15.7 ± 0.3	−12.3 ± 3.5
k_{1c}, M^{-1} s^{-1}	1241	1.4	1.7	0.22	38	0.17	5.0×10^{-2}	2.1	8.8×10^{-2}	2.8×10^{-2}
$\Delta H_{2c}^{\ddagger}$		23.4 ± 0.5	20.9 ± 0.4	20.6 ± 0.1						
$\Delta S_{2c}^{\ddagger}$		9.7 ± 1.7	0.9 ± 1.0	5.3 ± 0.4						
k_{2c}, s^{-1}		6.1×10^{-3}	4.2×10^{-3}	0.074						
$\Delta H_c°$		−10.3	−9.3	−9.0						
$\Delta S_c°$		−23.6	−19.5	−27.8						
K_c, M^{-1}		230	405	3.0						
$\Delta H_{3c}^{\ddagger}$	19.9 ± 0.1	21.3 ± 0.2	23.3 ± 0.1	23.7 ± 0.2		24.3 ± 0.6	23.5 ± 0.2		27.4 ± 0.8[b]	
$\Delta S_{3c}^{\ddagger}$	8.4 ± 0.2	6.1 ± 0.6	13.6 ± 0.2	13.9 ± 0.5	*f*	9.1 ± 2.1	6.6 ± 0.7	*f*	12.8 ± 0.5	*f*
k_{3c}, s^{-1}	1.13	3.2×10^{-2}	5.0×10^{-2}	2.9×10^{-2}		9.2×10^{-4}	1.0×10^{-3}		3.05×10^{-5}	

[a] TTP = $P\{(2,4,6\text{-}OMe)_3C_6H_2\}_3$. [b] Reference 1d. [c] References 11 and 12. [d] All ΔH values in kcal mol^{-1}. [e] All ΔS values in cal mol^{-1} K^{-1}. [f] Decomposition occurred.

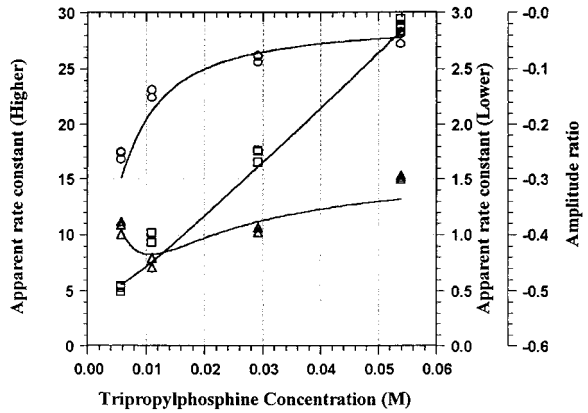

Figure 4. Dependence of the observed rate constants and the amplitude ratio on phosphine concentration for the reaction of **2** with PPr^n_3 at 25 °C. Squares represent the lower rate constant, circles represent the higher rate constant, and triangles represent the ratio of the amplitudes. The solid line depicts the calculated fit to all of the points, based on the parameters in Table 1.

rate constants for the two steps greatly diverged, as described in the Experimental Section. A variety of patterns can be observed in the data in Table 1. The dependence on phosphine is demonstrated most extensively for the reactions of **2**. The values of k_{1m} and its attendant activation parameters vary little. Considering only k_{1m}(25 °C), PMe_3 is somewhat more reactive than the other phosphines, but there is little variation in the activation parameters. When there is some variation in the activation parameters, as with $PMePh_2$, they compensate, leaving the k_{1m}(25 °C) values little different. There is a significant increase in k_{2m}, due to a decrease in $\Delta H^{\ddagger}$, with decreasing pK_a of the phosphine. This trend is most clearly seen when k_{1m} and k_{2m} are combined to give K_m, the equilibrium constant for the formation of the intermediate from the reactants. Excluding the exceptionally bulky and generally differently reacting ortho-substituted phenylphosphine $P\{(2,4,6\text{-}OMe)_3C_6H_2\}_3$,[23] there is a decrease in stability of the intermediate with decreasing basicity of the ligand. The origin of this trend is primarily in $\Delta H_m°$. The fact that the k_{1m} step is hardly affected by both size and basicity of the entering phosphine suggests that ring slippage and concomitant ligand rearrangements occur to a large extent prior to Ru−P bond formation. This may be interpreted as a rapid preequilibrium between η^5 and η^3 forms of the starting complexes **2**−**4**, where the latter react in a rate-determining step with the entering phosphine to give the stable η^3 complexes **6**−**8** (Scheme 8). Thus, the unsaturated η^3 species $[Ru(\eta^3\text{-}C_5H_5)(\eta^4\text{-}C_5H_4O)(L)]^+$ lies near in energy to the transition state where, as depicted in Figure 5, Ru−P bond formation is incomplete. Similar observations have been made in ring slippage processes involving the indenyl ligand.[24,31] The k_{2m} pathway, on the other hand, requires the cleavage of a strong Ru−P bond. Although there are no absolute Ru−P bond dissociation energies available in the literature, the activation enthalpies for PMe_3 dis-

Scheme 8

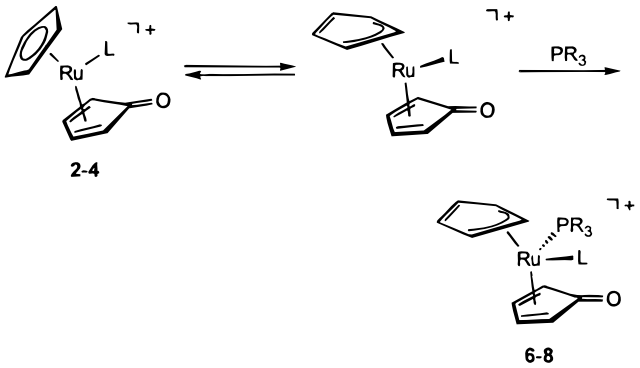

(23) (a) Atton, J. G.; Kane-Maguire, L. A. P. *J. Chem. Soc., Dalton Trans.* **1982**, 1491. (b) Chapman, S.; Kane-Maguire, L. A. P. *J. Chem. Soc., Dalton Trans.* **1995**, 2021.

(24) Calhorda, M. J.; Gamelas, C. A.; Gonçalves, I. S.; Herdtweck, E.; Romão, C. C.; Veiros, L. F. *Organometallics* **1998**, *17*, 2597.

(25) Bryndza, H. E.; Domaille, P. J.; Paciello, R. A.; Bercaw, J. E. *Organometallics* **1989**, *8*, 379.

(26) Gemel, C.; Kalt, D.; Sapunov, V. N.; Mereiter, K.; Schmid, R.; Kirchner, K. *Organometallics* **1997**, *16*, 427.

(27) Breulet, J.; Lee, T. J.; Schaefer, H. F., III *J. Am. Chem. Soc.* **1984**, *106*, 6250.

(28) Hughes, R. P.; Rose, P. R.; Zheng, X.; Rheingold, A. L. *Organometallics* **1995**, *14*, 2407

(29) (a) Margl, P.; Schwarz, K. *J. Chem. Phys.* **1995**, *103*, 683. (b) Anh, N. T.; Elian, M.; Hoffmann, R. *J. Am. Chem. Soc.* **1978**, *100*, 110. (c) Shen, J. K.; Thang, S. Z.; Basolo, F.; Johnson, S. E.; Hawthorne, M. F. *Inorg. Chim. Acta* **1995**, *235*, 89

(30) Huttner, G.; Brintzinger, H. H.; Bell, L. G.; Friderich, P.; Bejenke, V.; Neugebauer, D. *J. Organomet. Chem.* **1978**, *145*, 329.

(31) Rerek, M. E.; Basolo, F. *Organometallic* **1983**, *2*, 372.

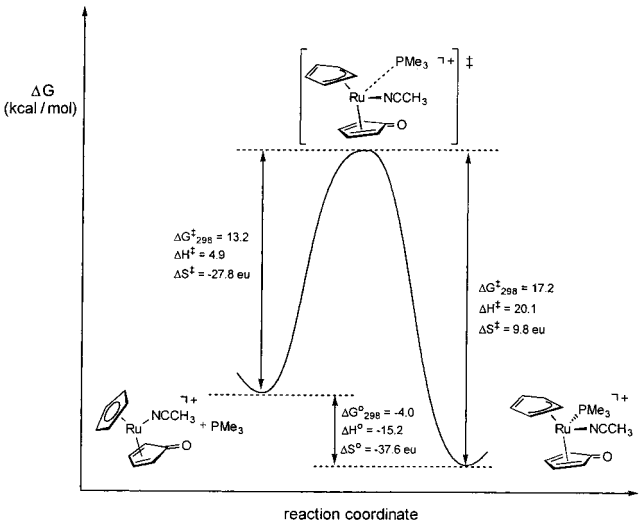

Figure 5. Reaction coordinate diagram for the conversion of **2** to **6a**.

sociation from $Ru(\eta^5\text{-}C_5Me_5)(PMe_3)_2X$ (X = various anionic N, S, and C donor ligands and halides) provide approximate minimum Ru−P bond strengths which are on the order of 23−47 kcal mol^{-1}.[25] The strength of the Ru−P bond in **6**−**8** appears to follow the order $PMe_3 \approx PBu^n_3 > PMe_2Ph > PMePh_2 > PPh_3$, which parallels their basicities.

The product formation step, like the initial bimolecular attack, is little affected by changes in the ligand for the four ligands that give this rate constant. However, the upper limit on the rate constant estimated for k_{3m} from $PMePh_2$ indicates that this process is much slower for the least basic ligand for which attack at Ru is observed.

The dependence of the reactivity on the ancillary ligand L is demonstrated most completely for the reactions of **3**. The bimolecular step, k_{1m}, has a lower rate constant primarily due to an increased activation enthalpy. The values of k_{2m} and K_m are quite similar to those for the reactions of **2**, with the trend to decreased stability of the intermediate with decreasing basicity slightly more pronounced than in the first case. These compounds do not continue to product, thus showing a large but unmeasurable decrease in k_{3m}. The change of L from pyridine to thiourea gives a further decrease in reactivity with PMe_3 (k_{1m}) and a similar k_{2m}, thus a yet less stable intermediate. The observed effect of the ligands L may be explained by their nucleophilicity with respect to the $[Ru(\eta^5\text{-}C_5H_5)(\eta^4\text{-}C_5H_4O)]^+$ fragment taken to increase in the order C_5H_4O (**1**) < CH_3CN (**2**) < pyridine (**3**) < thiourea (**4**).[15] It should be noted that none of these ancillary ligands are sterically demanding (Figures 1 and 2). Therefore, the reactivity of **1**−**4** toward phosphines in the order **1** > **2** > **3** > **4** is probably not due to significant steric contributions.

This study has also produced further kinetic data on phosphines that attack directly at the C_4H_4O ligand, producing 1,2-disubstituted ruthenocenes **13**. The new results and those from the first paper in this series[3d] are presented in Table 2. The addition of the bulky and basic $P\{(2,4,6\text{-}OMe)_3C_6H_2\}_3$ demonstrates a trend in the bimolecular process, k_{1c}, that was not present in the bimolecular attack at Ru, k_{1m}. The rate constant decreases as the basicity of the phosphine decreases with no sensitivity to cone angle. This is true for all three ancillary ligands. The change from CH_3CN to pyridine and then to thiourea produces a progressive decrease in the rate constant due to changes in both enthalpy and entropy of activation, with the enthalpy effect usually dominating, but $P\{(2,4,6\text{-}OMe)_3C_6H_2\}_3$ shows more complex changes. New data on the product formation step, k_{3c}, also demonstrate some trends. The largest and most basic phosphine, $P\{(2,4,6\text{-}OMe)_3C_6H_2\}_3$, leads to the fastest reaction when CH_3CN is being expelled. For the comparisons that can be made, in reactions with PMe_2Ph and $PMePh_2$, the ancillary ligands pyridine and thiourea slow the reaction compared to CH_3CN.

A major question to be answered is the origin of the change in product with a change in the entering phosphine. Only the more basic phosphines react to produce the C_5H_5-modified 1,1′-disubstituted ruthenocene. The question remains as to why the more basic phosphines do not also produce the product of attack at C_5H_4O, the 1,2-disubstituted product. Some indication comes from the reaction of $PMePh_2$, which produces both intermediates but only the 1,2-disubstituted product. These data were obtained by studying the reactions at different temperatures. Considering the rate constants at 25 °C, the reaction to form intermediate **6d**, the result of attack at Ru, is 300-fold faster than the reaction to form intermediate **9d**, in which attack has occurred at C_5H_4O. However, the reverse reactions of these two processes show an even greater disparity. Thus the equilibrium constant for the formation of **6d** is only 0.8 M^{-1}, while for the formation of **9d** it is 230 M^{-1}. The conversion of **6d** to product could not be observed, while **9d** is converted to product with a rate constant (k_{3c}) similar to that of all phosphines showing this reactivity. The trend in k_{3m} with phosphine basicity, if it extrapolates to $PMePh_2$, would give a rate constant lower than that of the other phosphines but comparable to k_{3c}. Thus the kinetics indicate that both the stability of the intermediate and, to a lesser extent, the lower reactivity in the product-forming step prevents the less basic phosphines from giving the 1,1′-product. Conversely, the enhanced stability of the intermediate formed from phosphine attack at Ru and the enhanced reactivity in the product-forming step for the more basic phosphines lead to the 1,1′-disubstituted product from these nucleophiles.

In the presence of excess $PR_3 = PMe_3$ and $Me_2PCH_2PMe_2$, the η^3-intermediates **7** and **8** proceed by a different pathway to yield **14** and **15**, respectively, together with free $C_5H_4PR_3$ (Scheme 3). The kinetics of the reaction of **7a** with PMe_3 have been studied by means of ^1H NMR spectroscopy as described in the Experimental Section. A simple second-order rate law, first order in each reactant, was obtained. The apparent second-order rate constant k_{4m} at 25 °C is 2.4×10^{-2} M^{-1} s^{-1} with $\Delta H^‡$ of 13.8 ± 1.2 kcal mol^{-1} and $\Delta S^‡$ of −19.8 ± 4.5 cal mol^{-1} K^{-1}. The activation parameters are indicative of an associative process. However, the overall process requires two phosphines, and thus it is unclear what process or combination of processes is actually being observed.

As has been previously shown,[15] CH_3CN in **2** is readily substituted by pyridine to give **3** quantitatively. To establish whether this reaction proceeds via an

Scheme 9

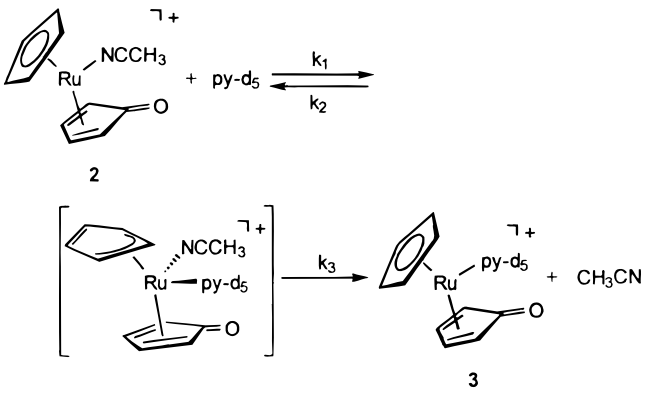

associative pathway, i.e., via an η^3-C_5H_5 intermediate, the kinetics of this reaction were studied by ^{1}H NMR spectroscopy (Scheme 9). A simple second-order rate law, first order in each reactant was obtained. The apparent second-order rate constant at 25 °C is 1.6×10^{-3} M^{-1} s^{-1} with a $\Delta H^{\ddagger}$ of 18.3 ± 0.4 kcal mol^{-1} and $\Delta S^{\ddagger}$ of −10.0 ± 1.4 cal mol^{-1} K^{-1}. These data are consistent with a bimolecular mechanism involving coordination of pyridine-d_5 to the ruthenium center concomitant with an η^5 to η^3 ring slip of the C_5H_5 ligand, followed by dissociation of the CH_3CN ligand (Scheme 7). Again the simplicity of the rate law does not allow further information concerning the individual rate constants to be obtained from the data.

EHMO Calculations. An insight into a possible mechanism of the two reaction pathways is provided by extended Hückel molecular orbital calculations. The LUMO and SLUMO of $[Ru(\eta^3\text{-}C_5H_5)(\eta^4\text{-}C_5H_4O)(L)]^+$ having the characteristics of the π^* MO of C_5H_4O and that of the second e_{1g} of C_5H_5, respectively, are relevant to nucleophilic attack by PR_3 at the C_5H_4O ligand and at the metal. In the ground state, however, both modes of attack are not possible without a prior change in orbital symmetries through ligand rearrangement. Furthermore, the LUMO (for attack at C_5H_4O) and the SLUMO (for attack at the metal) lie too high in energy and the overlap integral between these MO's and the σ PR_3 orbital is too small. It has to be noted also that the reactivity of $[Ru(\eta^5\text{-}C_5H_5)(\eta^3\text{-}C_5H_4O\text{-}PR_3)(L)]^+$ is affected by L since its π^* and/or σ orbitals participate in the SLUMO and the LUMO, respectively. Thus, strong π-acceptor and σ-donor ligands disfavor both modes of nucleophilic attack in agreement with the kinetic data.

To provide better interactions between the nucleophile and the C_5H_4O ring, the LUMO of the Ru complex must be altered to include the p_z orbital of the C_5H_4O α-carbons and to lower its energy. This is affected by η^4 to η^3 ring slippage and subsequent gauche deformation of the C_5H_4O ligand similar to the transition state suggested by us previously for the nucleophilic attack at acyclic 1,3-diene ligands.[26] For free 1,3-butadiene, it is noteworthy that the gauche structure is only about 0.4 kcal mol^{-1} higher in energy than the s-cis structure.[27] In the case of hexafluoro-1,3-butadiene, the gauche conformer was even shown to be the ground-state structure.[28] This interaction should be little affected by the shape and size of PR_3 but should be sensitive to the nucleophilicity of the phosphine (see kinetics data). It should be re-emphasized here that attack at C_5H_4O does not need prior reduction in the metal valence electron count.

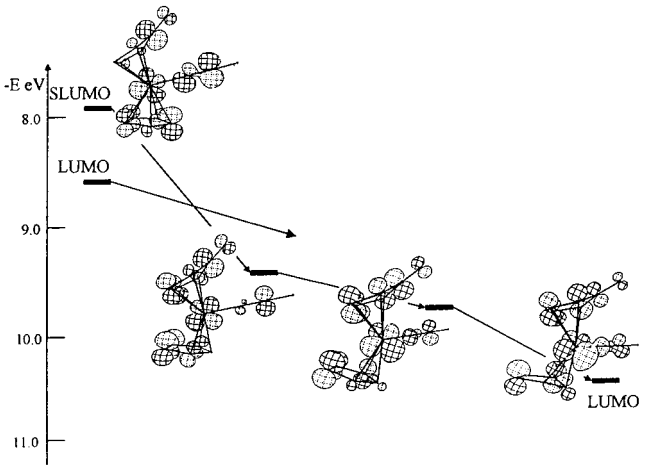

Figure 6. $\eta^5 \rightarrow \eta^3$ ring slippage and concomitant ligand rearrangements of **2**: CACAO drawing for the SLUMO−LUMO inversion (in the absence of the nucleophile).

Attack at the metal center requires geometric changes toward a 16-electron intermediate in which the SLUMO has lower energy. Otherwise, an energetically unfavorable 20-electron complex has to be formed. The following proposal, shown in Figure 6, is appealing: The six-electron donor C_5H_5 can be transformed into a four-electron donor through $\eta^5 \rightarrow \eta^3$ ring slippage, thus affording a 16-electron complex and promoting metal attack. For the formation of $[Ru(\eta^3\text{-}C_5H_5)(\eta^4\text{-}C_5H_4O)(CH_3CN)(PR_3)]^+$, in addition to formation of the 16e complex and the decrease in the SLUMO level, of primary importance is the availability of a vacant low-lying metal-centered orbital for the entry of PR_3. Computer simulations of the positional changes of the ligands C_5H_4O and CH_3CN (slipping, folding, bending) show that the change in the orbital symmetry at the metal center is highly unfavorable energetically. For the C_5H_5 ligand, both rotation and $\eta^5 \rightarrow \eta^3 \rightarrow \eta^1 \rightarrow \eta^3 \rightarrow \eta^5$ ring-slippage barriers are known to be very low (at least in the absence of any ring deformations[29]) but to be ineffective as regards orbital symmetry changes. However, $\eta^5 \rightarrow \eta^3$ slippage can provoke ring deformation affording an allyl system that typically leads to a bent η^3-C_5H_5 ligand with a dihedral angle of about 20°.[30] Such a rearrangement creates a vacant orbital at the metal and may provide a low-energy associative reaction path.[31] This is also characteristic of the indenyl system.[24,32] In the present case, the 16e complex is formed with SLUMO−LUMO inversion. Although the new LUMO level is lowered by C_5H_5−Ru bond weakening, there is no orbital of suitable symmetry for nucleophilic attack at Ru to occur unless there are a horizontal swing of CH_3CN and concomitant rotation of the η^3-C_5H_5 system to improve the conjugation in the final complex fragment (in the absence of the nucleophile). The new MO (the LUMO of the 16e complex) is a low-lying metal-centered orbital suitable for attack by PR_3.

Conclusion

There is an increasing awareness of the importance of haptotropic rearrangement reactions of polyenyl

(32) Kowaleski, R. M.; Rheingold, A. L.; Trogler, W. C.; Basolo, F. *J. Am. Chem. Soc.* **1986**, *108*, 2460.

ligands which become facile processes when certain conditions are met. In the present case, the $\eta^5 \rightarrow \eta^3$ ring slippage of the C_5H_5 ligand is promoted with the aid of the coligand cyclopentadienone, which acts as a "built-in" oxidizing agent converting into an η^5-bound oxocyclopentadienyl ligand. This may be called the cyclopentadienone effect, similar to the known indenyl effect. The energy barrier for $\eta^5 \rightarrow \eta^3$ ring slippage of the indenyl ligand is extremely low since the fused benzo ring regains its full aromaticity in the η^3 coordination mode.

At first glance, one would surmise that the present conversion of the 18-electron complex $[Ru(\eta^5\text{-}C_5H_5)(\eta^4\text{-}C_5H_4O)(L)]^+$ with tertiary phosphines to give stable η^3-C_5H_5 complexes of $[Ru(\eta^3\text{-}C_5H_5)(\eta^4\text{-}C_5H_4O)(L)(PR_3)]^+$ is driven by the Ru−P bond formation. However, the kinetic analysis shows that the ring slippage reaction is little affected by the entering nucleophile. This finding suggests ligand rearrangements to occur prior to Ru−P bond formation. As we have shown here, η^3-C_5H_5 and possibly η^1-C_5H_5 complexes are intermediates in the formation of substituted cyclopentadienyl products; i.e., ring slippage is a feasible way to activate C_5H_5 ligands toward nucleophilic attack.

Experimental Section

General Information. Manipulations were performed under an inert atmosphere of nitrogen by using standard Schlenk techniques and/or a glovebox. All chemicals were standard reagent grade and were used without further purification. The solvents were purified according to standard procedures.[33] The deuterated solvents were purchased from Aldrich and dried over 4 Å molecular sieves. $[Ru(\eta^5\text{-}C_5H_5)(\eta^4\text{-}C_5H_4O)]_2(CF_3SO_3)_2$ (**1**), $[Ru(\eta^5\text{-}C_5H_5)(\eta^4\text{-}C_5H_4O)(CH_3CN)]CF_3SO_3$ (**2**), $[Ru(\eta^5\text{-}C_5H_5)(\eta^4\text{-}C_5H_4O)(py)]CF_3SO_3$ (py = pyridine) (**3**), $[Ru(\eta^5\text{-}C_5H_5)(\eta^4\text{-}C_5H_4O)(tu)]CF_3SO_3$ (tu = thiourea) (**4**), $[Ru(\eta^5\text{-}C_5H_5)(CH_3CN)_3]PF_6$, and $NaBAr'_4$ ($Ar' = 3,5\text{-}C_6H_3(CF_3)_2$) were prepared according to the literature.[3,15,34] The intermediates $[Ru(\eta^5\text{-}C_5H_5)(\eta^3\text{-}C_5H_4O\text{-}PR_3)(CH_3CN)]^+$ (**9**), with the exception of $[Ru(\eta^5\text{-}C_5H_5)(\eta^3\text{-}C_5H_4O\text{-}PMePh_2)(CH_3CN)]^+$ (**9a**), were detected only kinetically. The NMR spectra of the intermediates $[Ru(\eta^5\text{-}C_5H_5)(\eta^3\text{-}C_5H_4O\text{-}PR_3)(py)]^+$ (PR_3 = PMe_3 (**10a**), PBu^n_3 (**10b**), PMe_2Ph (**10c**), $PMePh_2$ (**10d**)) and $[Ru(\eta^5\text{-}C_5H_5)(\eta^3\text{-}C_5H_4O{-}PR_3)(tu)]^+$ (PR_3 = PMe_3 (**11a**), PBu^n_3 (**11b**), PMe_2Ph (**11c**), $PMePh_2$ (**11d**)) have been described previously.[3d] Syntheses and NMR spectra of $[Ru(\eta^5\text{-}C_5H_4PR_3)(\eta^5\text{-}C_5H_4OH)]^+$ (PR_3 = PMe_3 (**12a**), PBu^n_3 (**12b**), PMe_2Ph (**12c**), $PMePh_2$ (**12d**), PPh_3 (**12e**), PCy_3 (**12f**)) and $[Ru(\eta^5\text{-}C_5H_5)(\eta^5\text{-}C_5H_3\text{-}2\text{-}PR_3{-}OH)]^+$ (PR_3 = PMe_3 (**13a**), PBu^n_3 (**13b**), PMe_2Ph (**13c**), $PMePh_2$ (**13d**), PPh_3 (**13e**), PCy_3 (**13f**)) have been reported elsewhere.[3] Infrared spectra were recorded on a Perkin-Elmer 16PC FT IR spectrometer. ^1H, $^{13}C\{^1H\}$, and $^{31}P\{^1H\}$ NMR spectra were recorded on a Bruker AC 250 spectrometer operating at 250.13, 62.86, and 101.26 MHz, respectively, and were referenced to $SiMe_4$ and to H_3PO_4 (85%). Temperature readings were calibrated by using the method of Raiford et al.,[35] corrected to 250.13 MHz, by adding a capillary of methanol to the experimental sample. The assignments of the proton resonances were aided by double-resonance experiments and $^1H-^1H$ shift correlated (COSY) spectra. Microanalyses were carried out by the Microanalytical Laboratories, University of Vienna.

Syntheses. $[Ru(\eta^5\text{-}C_5H_5)(\eta^4\text{-}C_5H_4O)(py)]BAr'_4$ (3′). 3 (155 mg, 0.327 mmol) and $NaBAr'_4$ (320 mg, 0.361 mmol) were dispersed in CH_2Cl_2 (15 mL), and the mixture was stirred for 1 h at room temperature, whereupon a precipitate of $NaCF_3SO_3$ formed. Solid materials were removed by filtration, and the solution was evaporated to dryness. The pale yellow solid was washed several times with diethyl ether to remove unreacted $NaBAr'_4$ and then dried under vacuum. Yield: 318 mg (82%). ^1H NMR (δ, CD_3CN, −35 °C): 8.70 (d, 2H, py), 7.59 (t, 1H, py), 7.72 (b s, 8H, Ar′), 7.65 (s, 4H, Ar′), 7.47 (t, 2H, py), 6.15 (t, 2H), 5.44 (s, 5H, C_5H_5), 4.51 (t, 2H).

$[Ru(\eta^5\text{-}C_5H_5)(\eta^4\text{-}C_5H_4O)(tu)]BAr'_4$ (4′). This compound was synthesized analogously to **3′** by treatment of **4** with $NaBAr'_4$ in CH_2Cl_2. ^1H NMR (δ, CD_3CN, −35 °C): 7.70 (b s, 8H, Ar′), 7.64 (s, 4H, Ar′), 7.30 (b s, 2H, tu), 6.84 (b s, 2H, tu), 5.96 (b s, 2H), 5.46 (s, 5H, C_5H_5), 4.13 (b s, 2H).

NMR Spectroscopic Studies. Typically, a 5 mm NMR tube was charged with a solution of either **1**, **2**, **3** (**3′**), or **4** (**4′**) (ca. 20−30 mg) in neat acetone-d_6, CD_3NO_2, or a mixture thereof (0.5 mL) and was capped with a septum. The tube was then cooled to an appropriate temperature, and the tertiary phosphine (ca. 1 equiv) was added by syringe. In the case of solid phosphines, the NMR tube was charged with complexes **1**−**4** and the tertiary phosphine and the sample was cooled to an appropriate temperature. Deuterated solvent was then added slowly by syringe. The sample was transferred to a precooled NMR probe, and ^1H and $^{31}P\{^1H\}$ NMR spectra were immediately recorded. $^{13}C\{^1H\}$ NMR spectra were recorded when the stability of the complexes allowed.

Reaction of 1 with PMe_3. Formation of $[Ru(\eta^3\text{-}C_5H_5)(\eta^4\text{-}C_5H_4O)(PMe_3)]_2(CF_3SO_3)_2$ (5a). ^1H NMR (δ, acetone-d_6, −70 °C): 5.68 (m, 2H), 4.76 (m, 1H), 4.66 (m, 1H), 4.60 (m, 1H), 4.43 (m, 1H), 4.32 (m, 1H), 4.08 (m, 1H), 3.84 (m, 1H), 1.83 (d, 9H, $^2J_{HP}$ = 14.3 Hz). $^{13}C\{^1H\}$ NMR (δ, CD_3NO_2/acetone-d_6 (1:1), −70 °C): 166.3 (C═O), 80.1, 79.6, 76.1, 75.5, 73.1, 71.4, 56.8, 56.3, 48.9 (d, J_{CP} = 20.8 Hz), 6.3 (d, J_{CP} = 50.3 Hz, PMe_3). $^{31}P\{^1H\}$ NMR (δ, acetone-d_6, −70 °C): 26.4. At temperatures above −50 °C, quantitative formation of **12a** was observed.

Reaction of 1 with PCy_3. Formation of $[Ru(\eta^3\text{-}C_5H_5)(\eta^4\text{-}C_5H_4O)(PCy_3)]_2(CF_3SO_3)_2$ (5b). ^1H NMR (δ, acetone-d_6, −78 °C): 5.79 (m, 2H), 4.80 (m, 1H), 4.65 (m, 2H), 4.52 (m, 1H), 4.46 (m, 1H), 4.28 (m, 1H), 3.99 (m, 1H), 2.63 (m, 3H), 2.00−1.20 (m, 30H). $^{31}P\{^1H\}$ NMR (δ, acetone-d_6, −78 °C): 31.9. At temperatures above −50 °C, quantitative formation of **12f** was observed.

Reaction of 1 with $P\{(2,4,6\text{-}OMe)_3C_6H_2\}_3$. Formation of $[Ru(\eta^3\text{-}C_5H_5)(\eta^4\text{-}C_5H_4O)(P\{(2,4,6\text{-}OMe)_3C_6H_2\}_3)]_2(CF_3SO_3)_2$ (5c). ^1H NMR (δ, acetone-d_6, −78 °C): 6.35−6.10 (m, 6H), 5.66 (m, 2H), 5.04 (m, 1H), 4.89 (m, 1H), 4.72 (m, 1H), 4.60 (m, 1H), 4.46 (m, 1H), 4.33 (m, 1H), 3.90−3.30 (m, 28H). The resonance of one of the η^3-C_5H_5 protons was obscured by those of the $P\{(2,4,6\text{-}OMe)_3C_6H_2\}_3$ ligand. $^{31}P\{^1H\}$ NMR (δ, acetone-d_6, −78 °C): 6.5. At temperatures above −50 °C, quantitative formation of $[Ru(\eta^5\text{-}C_5H_4P\{(2,4,6\text{-}OMe)_3C_6H_2\}_3)(\eta^5\text{-}C_5H_4OH)]^+$ (**12g**) was observed. ^1H NMR for **12g** (δ, acetone-d_6, 20 °C): 6.31 (d, 9H, J = 4.6 Hz), 4.63 (m, 2H), 4.58 (m, 2H), 4.51 (m, 4H), 3.91 (s, 18H), 3.83 (s, 9H). $^{31}P\{^1H\}$ NMR for **12g** (δ, acetone-d_6, 20 °C): 1.0.

Reaction of 1 with PPh_3. Formation of $[Ru(\eta^3\text{-}C_5H_5)(\eta^4\text{-}C_5H_4O)(PPh_3)]_2(CF_3SO_3)_2$ (5d). ^1H NMR (δ, acetone-d_6, −90 °C): 5.51 (m, 1H), 5.46 (m, 1H), 5.38 (m, 1H), 4.95 (m, 1H), 4.89 (m, 1H), 4.82 (m, 1H), 4.74 (m, 1H), 4.54 (m, 1H), 4.48 (m, 1H). The resonances of the PPh_3 ligand are superimposed by the resonances of the free PPh_3 ligand. $^{31}P\{^1H\}$ NMR (δ, acetone-d_6, −90 °C): 19.5. At temperatures above −50 °C, quantitative formation of **12e** was observed.

Reaction of 1 with $Me_2PCH_2PMe_2$. Formation of $[Ru(\eta^3\text{-}C_5H_5)(\eta^4\text{-}C_5H_4O)(\eta^1(P)\text{-}Me_2PCH_2PMe_2)]_2(CF_3SO_3)_2$ (5e). ^1H NMR (δ, acetone-d_6, −81 °C): 5.65 (m, 2H), 4.73 (m, 1H), 4.67 (m, 1H), 4.60 (m, 1H), 4.45 (m, 1H), 4.28 (m, 1H), 4.10

(33) Perrin, D. D.; Armarego, W. L. F. *Purification of Laboratory Chemicals*, 3rd ed.; Pergamon: New York, 1988.
(34) Brookhart, M.; Grant, B.; Volpe, J. *Organometallics* **1992**, *11*, 3920.
(35) Raiford, D. S.; Fisk, C. L.; Becker, E. D. *Anal. Chem.* **1979**, *51*, 1, 2050.

(m, 1H), 3.81 (m, 1H), 1.76 (d, 6H, $^2J_{HP}$ = 13.5 Hz, PMe_2), 1.34 (t, 2H, $^2J_{HP}$ = 3.2 Hz, PCH_2P), 0.97 (d, 6H, $^2J_{HP}$ = 8.4 Hz, PMe_2). $^{31}P\{^1H\}$ NMR (δ, acetone-d_6, −81 °C): 29.5 (d, $^2J_{PP}$ = 35.9 Hz), −43.4 (d, $^2J_{PP}$ = 35.9 Hz).

Reaction of 2 with PMe_3. Formation of [Ru(η^3-C_5H_5)(η^4-C_5H_4O)(PMe_3)(CH_3CN)]CF_3SO_3 (6a). ^1H NMR (δ, acetone-d_6, −90 °C): 5.63 (m, 2H, $H^{3,4}$), 4.95 (m, 2H, $H^{7,8}$), 4.32 (m, 1H, H^1), 3.93 (m, 2H, $H^{6,9}$), 3.81 (m, 2H, $H^{2,5}$), 3.66 (s, 3H), 1.76 (d, 9H, $^2J_{HP}$ = 14.4 Hz).$^{13}C\{^1H\}$ NMR (δ, acetone-d_6, −90 °C): 173.7 (C═O), 129.4 (CN), 78.3, 75.6, 65.8, 52.4 (d, J_{CP} = 5.3 Hz), 50.4 (d, J_{CP} = 14.8 Hz), 5.4 (d, J_{CP} = 54.1 Hz, PMe_3). $^{31}P\{^1H\}$ NMR (δ, acetone-d_6, −90 °C): 24.6. At temperatures above −50 °C, quantitative formation of **12a** was observed.

Reaction of 2 with PBu^n_3. Formation of [Ru(η^3-C_5H_5)(η^4-C_5H_4O)(PBu^n_3)(CH_3CN)]CF_3SO_3 (6b). ^1H NMR (δ, acetone-d_6, −90 °C): 5.66 (m, 2H, $H^{3,4}$), 4.92 (m, 2H, $H^{7,8}$), 4.35 (s, 1H, H^1), 3.96 (m, 2H, $H^{6,9}$), 3.80 (m, 2H, $H^{2,5}$), 2.18 (m, 6H), 1.60−1.20 (m, 12H), 0.87 (t, 9H).$^{13}C\{^1H\}$ NMR (δ, acetone-d_6, −90 °C): 173.8 (C═O), 129.8 (CN), 78.3, 75.9, 66.1, 53.0, 49.2 (d, J_{CP} = 13.9 Hz), 25.3 (d, J_{CP} = 15.3 Hz, PBu_3), 24.5, 17.8, 17.1, 5.4 (CH_3CN). $^{31}P\{^1H\}$ NMR (δ, acetone-d_6, −90 °C): 27.5. At temperatures above −50 °C, quantitative formation of **12b** was observed.

Reaction of 2 with PMe_2Ph. Formation of [Ru(η^3-C_5H_5)(η^4-C_5H_4O)(PMe_2Ph)(CH_3CN)]CF_3SO_3 (6c). ^1H NMR (δ, acetone-d_6, −70 °C): 8.00−7.60 (m, 5H), 5.19 (m, 2H, $H^{3,4}$), 4.80 (m, 2H, $H^{7,8}$), 4.45 (m, 1H, H^1), 3.85 (m, 2H, $H^{6,9}$), 3.71 (m, 2H, $H^{2,5}$), 2.60 (s, 3H), 2.21 (d, 6H, $^2J_{HP}$ = 13.7 Hz). $^{31}P\{^1H\}$ NMR (δ, acetone-d_6, −70 °C): 22.2. At temperatures above −50 °C, quantitative formation of **12c** was observed.

Reaction of 2 with $PMePh_2$. Formation of [Ru(η^3-C_5H_5)(η^4-C_5H_4O)($PMePh_2$)(CH_3CN)]CF_3SO_3 (6d) and [Ru(η^5-C_5H_5)(η^3-C_5H_4O-2-$PMePh_2$)(CH_3CN)]CF_3SO_3 (9a). The ^1H NMR spectrum was immediately recorded showing the formation of both [Ru(η^3-C_5H_5)(η^4-C_5H_4O)($PMePh_2$)(CH_3CN)]-CF_3SO_3 (**6d**) and [Ru(η^5-C_5H_5)(η^3-C_5H_4O-2-$PMePh_2$)(CH_3CN)]-CF_3SO_3 (**9a**). ^1H NMR for **6d** (δ, acetone-d_6, −90 °C): 8.00−7.60 (m, 10H, $PMePh_2$), 5.22 (m, 2H), 5.13 (m, 1H), 4.86 (m, 2H), 3.92 (m, 2H), 3.80 (m, 2H), 2.70 (s, 3H), 2.54 (d, 3H, J_{HP} = 13.9 Hz, $PMePh_2$). ^1H NMR for **9a** (δ, acetone-d_6, −90 °C): 8.00−7.60 (m, 10H), 5.49 (m, 1H), 4.70 (s, 5H), 4.11 (d, 1H, J_{HP} = 10.5 Hz), 3.67 (m, 1H), 3.52 (m, 1H), 2.61 (s, 3H), 2.60 (d, 3H, J_{HP} = 13.9 Hz, $PMePh_2$). When the solution was warmed to ambient temperature, only the resonances of **13d** and free CH_3CN were observed.

Reaction of 2 with P{(2,4,6-$OMe)_3C_6H_2$}$_3$. Formation of [Ru(η^5-C_5H_5)(η^5-C_5H_3OH-2-P{(2,4,6-$OMe)_3C_6H_2$}$_3$)]CF_3SO_3 (13g). ^1H NMR (δ, CD_3CN, 20 °C): 6.21 (d, 6H, J = 4.6 Hz), 4.70 (m, 1H), 4.41 (s, 5H), 4.39 (m, 1H), 4.25 (m, 12H), 3.87 (s, 9H), 3.45 (s, 18H). $^{31}P\{^1H\}$ NMR (δ, CD_3CN, 20 °C): −3.7.

Reaction of 2 with $Me_2PCH_2PMe_2$. Formation of [Ru(η^3-C_5H_5)(η^4-C_5H_4O)(η^1(P)-$Me_2PCH_2PMe_2$)(CH_3CN)]-CF_3SO_3 (6e). ^1H NMR (δ, acetone-d_6, −70 °C): 5.59 (m, 2H, $H^{3,4}$), 4.91 (m, 2H, $H^{7,8}$), 4.28 (s, 1H, H^1), 3.94 (m, 2H, $H^{6,9}$), 3.81 (m, 2H, $H^{2,5}$), 2.65 (s, 3H), 2.37 (d, 2H, J_{HP} = 14.5 Hz, PCH_2P), 1.76 (d, 6H, J_{HP} = 13.7 Hz, PMe_2), 1.17 (d, 6H, J_{HP} = 3.3 Hz, PMe_2). $^{13}C\{^1H\}$ NMR (δ, acetone-d_6, −70 °C): 173.8 (C═O), 129.5 (CN), 78.4, 75.8, 66.0, 52.5, 51.7 (d, J_{CP} = 17.6 Hz), 21.2 (dd, J_{CP} = 44.9 Hz, J_{CP} = 33.3 Hz, PCH_2P), 15.8 (dd, J_{CP} = 13.2 Hz, J_{CP} = 7.26 Hz, PMe_2), 5.2 (CH_3CN), 5.1 (dd, J_{CP} = 49.9 Hz, J_{CP} = 5.6 Hz, PMe_2). $^{31}P\{^1H\}$ NMR (δ, acetone-d_6, −70 °C): 27.5 (d, $^2J_{PP}$ = 41.3 Hz), −51.7 (d, $^2J_{PP}$ = 41.3 Hz).

Reaction of 2 with $Me_2PCH_2CH_2PMe_2$. Formation of [Ru(η^3-C_5H_5)(η^4-C_5H_4O)(η^1(P)-$Me_2PCH_2CH_2PMe_2$)(CH_3CN)]-CF_3SO_3 (6f). ^1H NMR (δ, acetone-d_6, −70 °C): 5.61 (m, 2H, $H^{3,4}$), 4.91 (m, 2H, $H^{7,8}$), 4.31 (s, 1H, H^1), 3.96 (m, 2H, $H^{6,9}$), 3.80 (m, 2H, $H^{2,5}$), 2.63 (s, 3H), 2.22 (b, 2H, PCH_2CH_2P), 1.76 (d, 6H, J_{HP} = 14.1 Hz, PMe_2), 1.58 (b, 2H, PCH_2CH_2P), 0.99 (s, 6H, PMe_2). $^{13}C\{^1H\}$ NMR (δ, acetone-d_6, −70 °C): 173.8 (C═O), 129.5 (CN), 78.3, 75.8, 66.0, 52.5, 50.4 (d, J_{CP} = 17.8 Hz), 20.9 (d, J_{CP} = 47.7 Hz, PCH_2CH_2P), 17.0 (dd, J_{CP} = 44.5 Hz, J_{CP} = 15.9 Hz, PCH_2CH_2P), 13.4 (d, J_{CP} = 13.4 Hz, PMe_2), 5.2 (CH_3CN), 3.6 (d, J_{CP} = 48.3 Hz, PMe_2). $^{31}P\{^1H\}$ NMR (δ, acetone-d_6, −70 °C):. 29.1 (d, $^3J_{PP}$ = 34.1 Hz), −43.7 (d, $^3J_{PP}$ = 34.1 Hz).

Reaction of 3 with PMe_3. Formation of [Ru(η^3-C_5H_5)(η^4-C_5H_4O)(PMe_3)(py)]CF_3SO_3 (7a). To a solution of **3** (200 mg, 0.422 mmol) in acetone-d_6 (5 mL) was added PMe_3 (0.86 mL, 0.844 mmol), resulting in the immediate formation of a pale yellow precipitate, which was collected on a glass frit, washed with diethyl ether, and dried under vacuum. Yield: 230 mg (99%). Anal. Calcd for $C_{19}H_{23}F_3NO_4RuS$: C, 41.46; H, 4.21; N, 2.54; P, 5.82. Found: C, 42.41; H, 4.30; N, 2.42; P, 5.63. ^1H NMR (δ, CD_3NO_2, −20 °C): 9.17 (m, 2H, py), 7.91 (m, 1H, py), 7.44 (m, 2H, py), 5.49 (m, 2H, $H^{3,4}$), 4.83 (m, 2H, $H^{7,8}$), 3.79 (m, 2H, $H^{6,9}$), 3.70 (m, 2H, $H^{2,5}$), 3.10 (m, 1H, H^1), 1.58 (d, 9H, $^2J_{HP}$ = 14.0 Hz). $^{13}C\{^1H\}$ NMR (δ, CD_3NO_2/acetone-d_6 (1:3), −20 °C): 173.7 (C═O), 160.6 (py), 139.1 (py), 127.3 (py), 78.0, 76.4, 68.3, 52.6 (d, J_{CP} = 5.1 Hz), 51.2 (d, J_{CP} = 19.9 Hz), 6.0 (d, J_{CP} = 49.5 Hz, PMe_3). $^{31}P\{^1H\}$ NMR (δ, CD_3NO, −20 °C): 30.7. At room temperature, formation of **12a** and **13a** was observed.

Reaction of 3 with PBu^n_3. Formation of [Ru(η^3-C_5H_5)(η^4-C_5H_4O)(PBu^n_3)(py)]CF_3SO_3 (7b). ^1H NMR (δ, CD_3NO_2/acetone-d_6 (1:3), −66 °C): 9.18 (m, 2H, py), 7.94 (m, 1H, py), 7.47 (m, 2H, py), 5.56 (m, 2H, $H^{3,4}$), 4.86 (m, 2H, $H^{7,8}$), 3.79 (m, 2H, $H^{6,9}$), 3.75 (m, 2H, $H^{2,5}$), 3.17 (m, 1H, H^1), 2.02 (m, 6H, PBu_3), 1.36 (m, 12H, PBu_3), 0.85 (m, 9H, PBu_3). $^{13}C\{^1H\}$ NMR (δ, CD_3NO_2/acetone-d_6 (1:3), −66 °C): 173.9 (C═O), 160.5 (py), 139.3 (py), 127.4 (py), 78.1, 76.5, 68.3, 53.2, 49.3 (d, J_{CP} = 12.5 Hz), 25.4 (d, J_{CP} = 15.3 Hz, PBu_3), 15.3 (s, PBu_3), 17.8 (d, J_{CP} = 42.5 Hz, PBu_3), 114.3 (s, PBu_3). $^{31}P\{^1H\}$ NMR (δ, CD_3NO_2/acetone-d_6 (1:3), −66 °C): 26.7. At room temperature, quantitative formation of **13b** was observed.

Reaction of 3 with PMe_2Ph. Formation of [Ru(η^3-C_5H_5)(η^4-C_5H_4O)(PMe_2Ph)(py)]CF_3SO_3 (7c). ^1H NMR (δ, acetone-d_6, −70 °C): 9.15 (m, 2H, py), 8.0−7.5 (m, 8H, py and PMe_2Ph), 5.19 (m, 2H, $H^{3,4}$), 4.83 (m, 2H, $H^{7,8}$), 3.72 (m, 2H, $H^{6,9}$), 3.65 (m, 2H, $H^{2,5}$), 3.57 (m, 1H, H^1), 2.08 (m, 9H, PMe_2Ph). $^{13}C\{^1H\}$ NMR (δ, acetone-d_6, −70 °C): 174.3 (C═O), 160.8 (py), 144.4 (d, J_{CP} = 13.9 Hz, PMe_2Ph), 139.2 (py), 135.5 (s, PMe_2Ph), 134.0 (d, J_{CP} = 9.3 Hz, PMe_2Ph), 130.8 (d, J_{CP} = 11.6 Hz, PMe_2Ph), 127.5 (py), 77.8, 76.5, 68.5, 53.4 (d, J_{CP} = 11.1 Hz), 51.9 (d, J_{CP} = 5.1 Hz), 5.1 (d, J_{CP} = 49.5 Hz, PMe_2Ph). $^{31}P\{^1H\}$ NMR (δ, acetone-d_6, −70 °C): 22.0. At room temperature, quantitative formation of **13c** was observed.

Reaction of 3 with PCy_3. Formation of [Ru(η^3-C_5H_5)(η^4-C_5H_4O)(PCy_3)(py)]CF_3SO_3 (7d). ^1H NMR (δ, acetone-d_6, −97 °C): 9.35 (m, 2H, py), 8.05 (m, 1H, py), 7.60 (m, 2H, py), 5.68 (m, 2H), 4.96 (m, 2H), 3.92 (m, 2H), 3.78 (m, 2H), 3.12 (m, 1H, H^1), 2.55 (m, 3H, PCy_3). The other resonances of PCy_3 were obscured by those of free PCy_3. $^{31}P\{^1H\}$ NMR (δ, acetone-d_6, −97 °C): 20.0. At room temperature, quantitative formation of **13f** was observed.

Reaction of 3 with $Me_2PCH_2PMe_2$. Formation of [Ru(η^3-C_5H_5)(η^4-C_5H_4O)(η^1(P)-$Me_2PCH_2PMe_2$)(py)] BAr'_4 (7e). ^1H NMR (δ, acetone-d_6, −47 °C): 9.20 (m, 2H, py), 7.95 (m, 1H, py), 7.82 (m, 8H, BAr'_4), 7.73 (m, 4H, BAr'_4), 7.48 (m, 2H, py), 5.57 (m, 2H, $H^{3,4}$), 4.91 (m, 2H, $H^{7,8}$), 3.77 (m, 2H, $H^{6,9}$), 3.72 (m, 2H, $H^{2,5}$), 3.34 (m, 1H, H^1), 2.29 (d, 2H, J_{HP} = 14.6 Hz, PCH_2P), 1.67 (d, 6H, J_{HP} = 13.6 Hz, PMe_2), 1.11 (d, 6H, J_{HP} = 3.4 Hz, PMe_2). $^{13}C\{^1H\}$ NMR (δ, acetone-d_6, −47 °C): 174.0 (C═O), 163.0 (BAr'_4, J_{CB} = 49.6 Hz), 160.6 (py), 139.0 (py), 135.9 (BAr'_4), 130.3 (BAr'_4, J_{CF} = 32.4 Hz), 127.2 (py), 125.7 (BAr'_4, J_{CF} = 272.0 Hz), 118.5 (BAr'_4), 77.5, 76.4, 68.4, 52.0, 51.8 (d, J_{CP} = 11.6 Hz), 21.9 (dd, J_{CP} = 44.6 Hz, J_{CP} = 32.6 Hz, PCH_2P), 16.0 (dd, J_{CP} = 13.2 Hz, J_{CP} = 7.2 Hz, PMe_2), 5.6 (dd, J_{CP} = 49.7 Hz, J_{CP} = 5.8 Hz, PMe_2). $^{31}P\{^1H\}$ NMR (δ, acetone-d_6, −47 °C): 27.5 (d, J_{PP} = 41.3 Hz), −52.3 (d, J_{PP} = 41.3 Hz).

Reaction of 3 with $Me_2PCH_2CH_2PMe_2$. Formation of $[Ru(\eta^3\text{-}C_5H_5)(\eta^4\text{-}C_5H_4O)(\eta^1(P)\text{-}Me_2PCH_2CH_2PMe_2)(py)]BAr'_4$ (7f). ^1H NMR (δ,acetone-d_6, −47 °C): 9.20 (m, 2H, py), 7.96 (m, 1H, py), 7.81 (m, 8H, BAr'_4), 7.72 (m, 4H, BAr'_4), 7.48 (m, 2H, py), 5.59 (m, 2H, $H^{3,4}$), 4.91 (m, 2H, $H^{7,8}$), 3.81 (m, 2H, $H^{6,9}$), 3.72 (m, 2H, $H^{2,5}$), 3.41 (m, 1H, H^1), 2.20 (m, 2H, PCH_2-CH_2P), 1.75 (d, 6H, J_{HP} = 13.9 Hz, PMe_2), 1.54 (m, 2H, PCH_2-CH_2P), 0.95 (d, 6H, J_{HP} = 2.4 Hz, PMe_2). $^{13}C\{^1H\}$ NMR (δ, acetone-d_6, −47 °C): 174.1 (C═O), 163.0 (BAr'_4, J_{CB} = 49.8 Hz), 160.6 (py), 139.0 (py), 135.9 (BAr'_4), 130.3 (BAr'_4, J_{CF} = 31.6 Hz), 127.9 (py), 125.7 (BAr'_4, J_{CF} = 272.0 Hz), 118.5 (BAr'_4), 77.6, 76.4, 68.4, 52.0 (d, J_{CP} = 5.1 Hz), 50.7 (d, J_{CP} = 14.8 Hz), 23.0 (dd, J_{CP} = 15.0 Hz, J_{CP} = 6.7 Hz, PCH_2CH_2P), 17.6 (dd, J_{CP} = 42.5 Hz, J_{CP} = 16.2 Hz, PCH_2CH_2P), 13.6 (d, J_{CP} = 13.9 Hz, P*Me*$_2$), 4.1 (d, J_{CP} = 48.6 Hz, P*Me*$_2$). $^{31}P\{^1H\}$ NMR (δ, acetone-d_6, −47 °C): 27.9 (d, J_{PP} = 34.1 Hz), −43.9 (d, J_{PP} = 34.1 Hz).

Reaction of 4 with PMe_3. Formation of $[Ru(\eta^3\text{-}C_5H_5)(\eta^4\text{-}C_5H_4O)(PMe_3)(tu)]CF_3SO_3$ (8a). PMe_3 (7.0 μL, 0.068 mmol) was added by syringe to a 5 mm NMR tube containing a sample of **4** (20 mg, 0.042 mmol) in CD_3NO_2 (0.5 mL) cooled at about −25 °C. The tube was placed into a precooled NMR probe at −20 °C, and quantitative formation of **7a** was observed. Attempts to isolate this complex in pure form, however, failed due to equilibrium reasons, and a mixture of **4** and **7a** was obtained in a 2:1 ratio. ^1H NMR (δ, CD_3NO_2, −20 °C): 8.39 (b, 4H, NH_2), 5.56 (m, 2H, $H^{3,4}$), 4.90 (m, 2H, $H^{7,8}$), 4.52 (m, 1H, H^1), 4.01 (m, 2H, $H^{6,9}$), 3.60 (m, 2H, $H^{2,5}$), 1.65 (d, 9H, $^2J_{HP}$ = 13.7 Hz). ^1H NMR (δ, CD_3NO_2, −20 °C): 8.40 (b, 4H, NH_2), 5.58 (m, 1H), 5.55 (m, 1H), 4.97 (m, 1H), 4.84 (m, 1H), 4.52 (m, 1H, H^1), 4.15 (m, 1H), 3.87 (m, 1H), 3.69 (m, 1H), 3.51 (m, 1H), 1.65 (d, 9H, $^2J_{HP}$ = 13.7 Hz). $^{31}P\{^1H\}$ NMR (δ, CD_3CN, −20 °C): 25.8. For solubility reasons, the $^{13}C\{^1H\}$ NMR (δ, CD_3CN, −20 °C) was recorded with $[Ru(\eta^3\text{-}C_5H_5)(\eta^4\text{-}C_5H_4O)(PMe_3)(tu)]BAr'_4$ (**8a′**): 182.8 (C═S), 171.6 (C═O), 162.3 (BAr'_4, J_{CB} = 49.4 Hz), 135.2 (BAr'_4), 129.3 (BAr'_4, J_{CF} = 31.3 Hz), 125.0 (BAr'_4, J_{CF} = 271.8 Hz), 76.0, 75.7, 74.3, 73.2, 67.5, 64.8, 52.8 (d, J_{CP} = 20.3 Hz), 50.3 (d, J_{CP} = 13.0 Hz), 47.0 (d, J_{CP} = 4.6 Hz), 5.7 (d, J_{CP} = 49.9 Hz, PMe_3). At room temperature, formation of **12a** and **13a** was observed.

Reaction of 4 with PBu^n_3. Formation of $[Ru(\eta^3\text{-}C_5H_5)(\eta^4\text{-}C_5H_4O)(PBu^n_3)(tu)]CF_3SO_3$ (8b). ^1H NMR (δ, CD_3NO_2/acetone-d_6 (1:1), −42 °C): 8.48 (b, 4H, NH_2), 5.58 (m, 1H, $H^{3,4}$), 5.53 (m, 1H, $H^{3,4}$), 4.92 (m, 1H), 4.81 (m, 1H), 4.73 (m, 1H, H^1), 4.13 (b, 1H), 3.81 (m, 1H), 3.67 (m, 1H), 3.51 (m, 1H). Resonances of the coordinated phosphine were obscured by those of free PBu^n_3. $^{31}P\{^1H\}$ NMR (δ, CD_3NO_2/acetone-d_6 (1:1), −42 °C): 27.2. At room temperature, quantitative formation of **13b** was observed.

Reaction of 4 with PMe_2Ph. Formation of $[Ru(\eta^3\text{-}C_5H_5)(\eta^4\text{-}C_5H_4O)(PMe_2Ph)(tu)]CF_3SO_3$ (8c). ^1H NMR (δ, CD_3NO_2, −12 °C): 8.27 (b, 4H, NH_2), 7.65−7.90 (m, 5H), 5.35 (m, 2H, $H^{3,4}$), 4.82 (m, 2H), 4.72 (d, 2H, $^2J_{HP}$ = 4.1 Hz), 3.90 (b, 2H), 3.54 (m, 2H), 2.02 (d, 6H, $^2J_{HP}$ = 13.5 Hz). $^{31}P\{^1H\}$ NMR (δ, CD_3NO_2, −41 °C): 20.4. At room temperature, quantitative formation of **13c** was observed.

Reaction of 4 with $Me_2PCH_2PMe_2$. Formation of $[Ru(\eta^3\text{-}C_5H_5)(\eta^4\text{-}C_5H_4O)(\eta^1(P)\text{-}Me_2PCH_2PMe_2)(tu)]CF_3SO_3$ (8d). ^1H NMR (δ, CD_3NO_2, −41 °C): 8.43 (b, 4H, NH_2), 5.54 (m, 2H, $H^{3,4}$), 4.96 (m, 1H), 4.84 (m, 1H), 4.61 (m, 1H, H^1), 4.04 (b, 1H), 3.87 (m, 1H), 3.69 (m, 1H), 3.51 (m, 1H), 2.11 (d, 2H, $^2J_{HP}$ = 13.5 Hz, PCH_2P), 1.69 (d, 6H, $^2J_{HP}$ = 13.4 Hz, PMe_2), 1.40 (s, 6H, PMe_2). $^{31}P\{^1H\}$ NMR (δ, CD_3NO_2, −41 °C): 26.5 (d, $^2J_{PP}$ = 44.9 Hz), −54.8 (d, $^2J_{PP}$ = 44.9 Hz).

Reaction of 4 with $Me_2PCH_2CH_2PMe_2$. Formation of $[Ru(\eta^3\text{-}C_5H_5)(\eta^4\text{-}C_5H_4O)(\eta^1(P)\text{-}Me_2PCH_2CH_2PMe_2)(tu)]CF_3SO_3$ (8e). ^1H NMR (δ, CD_3NO_2, −47 °C): 8.37 (b, 4H, NH_2), 5.59 (m, 1H, $H^{3,4}$), 5.55 (m, 1H, $H^{3,4}$), 4.97 (m, 1H), 4.85 (m, 1H), 4.62 (m, 1H, H^1), 4.05 (b, 1H), 3.87 (m, 1H), 3.70 (m, 1H), 3.52 (m, 1H), 2.08 (b, 2H, PCH_2CH_2P), 1.66 (d, 6H, $^2J_{HP}$ = 13.3 Hz, PMe_2), 1.54 (b, 2H, PCH_2CH_2P), 0.99 (d, 6H, $^2J_{HP}$ = 2.2 Hz, PMe_2). $^{31}P\{^1H\}$ NMR (δ, CD_3NO_2, −47 °C): 27.7 (d, $^3J_{PP}$ = 34.1 Hz), −46.1 (d, $^3J_{PP}$ = 34.1 Hz).

$[Ru(\eta^5\text{-}C_5H_4OH)(PMe_3)_2(py)]BAr'_4$ (14a). PMe_3 (20 μL, 0.20 mmol) was added by syringe to a 5 mm NMR tube containing a sample of **2** as the BAr'_4 salt (40 mg, 0.034 mmol) in acetone-d_6 (0.5 mL) cooled at about −30 °C. The tube was placed in a precooled NMR probe at −30 °C, and quantitative formation of **14a** and **16a** was observed within 12 h. ^1H NMR (δ, acetone-d_6, −30 °C): 8.72 (d, 2H, J = 5.14 Hz, py), 7.80 (m, 9H, BAr'_4, py), 7.70 (m, 4H, BAr'_4), 7.22 (t, 2H, J = 6.51 Hz, py), 4.14 (m, 4H, CPD), 1.54 (vt, 1H, J_{HP} = 3.77 Hz, PMe_3). The OH resonance was not observed. $^{13}C\{^1H\}$ NMR (δ, acetone-d_6, −30 °C): 163.0 (BAr'_4, J_{CB} = 49.9 Hz), 159.1 (py), 136.9 (py), 135.8 (BAr'_4), 130.3 (BAr'_4, J_{CF} = 29.6 Hz), 126.1 (py), 125.7 (BAr'_4, J_{CF} = 271.9 Hz), 118.5 (BAr'_4), 71.5, 61.0, 21.8 (t, J_{CP} = 13.9 Hz, PMe_3). The *C*O resonance was not observed. $^{31}P\{^1H\}$ NMR (δ, acetone-d_6, −30 °C): 9.1.

$[Ru(\eta^5\text{-}C_5H_4OH)(\eta^2(P,P)\text{-}Me_2PCH_2PMe_2)(py)]BAr'_4$ (14b). $Me_2PCH_2PMe_2$ (7 μL, 0.044 mmol) was added by syringe to a 5 mm NMR tube containing a sample of **2** as the BAr'_4 salt (25 mg, 0.021 mmol) in acetone-d_6 (0.5 mL) cooled at about −30 °C. The tube was kept at −30 °C for 12 h, after which it was transferred to a precooled NMR probe at −30 °C and quantitative formation of **14b** and **16b** was observed. ^1H NMR (δ, acetone-d_6, −30 °C): 8.88 (d, 2H, J = 5.4 Hz, py), 7.81 (m, 9H, BAr'_4, py), 7.73 (m, 4H, BAr'_4), 7.23 (t, 2H, J = 6.6 Hz, py), 4.17 (m, 4H), 3.66 (m, 2H, PCH_2P), 1.76 (vt, 6H, J_{HP} = 4.9 Hz, PMe_2), 1.54 (vt, 6H, J_{HP} = 4.9 Hz, PMe_2). The OH resonance was not observed. $^{31}P\{^1H\}$ NMR (δ, acetone-d_6, −30 °C): −15.9.

$[Ru(\eta^5\text{-}C_5H_4OH)(\eta^2(P,P)\text{-}Me_2PCH_2CH_2PMe_2)(py)]CF_3SO_3$ (14c). Monitoring of the formation of complex **14c** was carried out analogously to that for **14b**. ^1H NMR (δ, acetone-d_6, −30 °C): 8.69 (m, 1H, py), 8.57 (m, 1H, py), 7.75 (m, 1H, py), 7.39 (m, 1H, py), 7.18 (m, 1H, py), 4.41 (m, 2H), 3.92 (m, 2H), 1.70 (m, 6H, PMe_2), 1.44 (m, 3H, PMe) 1.35 (vt, 3H, J_{HP} = 3.5 Hz, PMe). The OH resonance was not observed, and the resonances of the PCH_2CH_2P moiety were obscured by the resonances of **16c**. $^{31}P\{^1H\}$ NMR (δ, acetone-d_6, −30 °C): −15.9.

$[Ru(\eta^5\text{-}C_5H_4OH)(PMe_3)_2(S{=}C(NH_2)_2)]CF_3SO_3$ (15). Monitoring of the formation of complex **15** was carried out analogously to that for **14b**. ^1H NMR (δ, CD_3NO_2, −20 °C): 4.26 (s, 2H), 4.19 (s, 2H), 1.46 (vt, 18H, J_{HP} = 4.2 Hz). The resonance of the OH proton could not be detected. $^{13}C\{^1H\}$ NMR (δ, CD_3NO_2, −20 °C): 185.8 (C═S), 126.4 (CO), 72.8, 61.3, 22.1 (t, J_{CP} = 14.8 Hz, PMe_3). $^{31}P\{^1H\}$ NMR (δ, CD_3NO_2, −20 °C): 8.0.

$C_5H_4PMe_3$ (16a). ^1H NMR (δ, acetone-d_6, −30 °C): 6.06 (m, 2H), 5.93 (m, 2H), 1.81 (d, 9H, J_{HP} = 13.7 Hz, Me). $^{13}C\{^1H\}$ NMR (δ, acetone-d_6, −30 °C): 113.1 (d, J_{CP} = 18.0 Hz), 112.2 (d, J_{CP} = 16.7 Hz), 13.6 (d, J_{CP} = 59.7 Hz, PMe_3). The resonance of the quaternary carbon could not be detected. $^{31}P\{^1H\}$ NMR (δ, acetone-d_6, −30 °C): 4.0 (cf. ref 14).

$C_5H_4PMe_2CH_2PMe_2$ (16b). ^1H NMR (δ, acetone-d_6, −30 °C): 6.07 (m, 2H), 5.94 (m, 2H), 1.92 (d, 6H, J_{HP} = 13.6 Hz, PMe_2), 0.74 (d, 6H, J_{HP} = 3.1 Hz, PMe_2). The resonances of the PCH_2P moiety were obscured by those of **14b**. $^{31}P\{^1H\}$ NMR (δ, acetone-d_6, −30 °C): 31.2 (d, J_{PP} = 50.3 Hz), 6.2 (d, J_{PP} = 52.1 Hz).

$[Ru(\eta^5\text{-}C_5H_5)(\eta^4\text{-}C_4H_6)(CH_3CN)]PF_6$ (17). A solution of $[Ru(\eta^5\text{-}C_5H_5)(CH_3CN)_3]PF_6$ (2.98 g, 6.86 mmol) in acetonitrile (300 mL) was saturated with 1,3-butadiene, and the mixture was heated at reflux for 35 min. During that time, the solution was purged several times with 1,3-butadiene. On removal of the solvent, a bright yellow solid was obtained, which was collected on a glass frit, washed with diethyl ether, and dried under vacuum. Yield: 1.26 g (45%). Anal. Calcd for $C_{11}H_{14}F_6NPRu$: C, 32.52; H, 3.47; N, 3.45. Found: C, 32.41; H, 3.30; N, 3.50. ^1H NMR (δ, acetone-d_6, −30 °C): 5.88 (m, 2H), 5.41 (s, 5H), 4.13 (d, 2H, J = 7.5 Hz), 2.64 (s, 3H), 1.52 (d, 2H, J = 9.8 Hz).

Table 3. Crystallographic Data

	3	**4**·CH_3CN	**18**
formula	$C_{16}H_{14}F_3NO_4RuS$	$C_{14}H_{16}F_3N_3O_4RuS_2$	$C_{15}H_{29}F_6P_3Ru$
fw	474.41	512.49	517.36
cryst size, mm	0.11 × 0.25 × 0.70	0.26 × 0.20 × 0.10	0.50 × 0.26 × 0.25
space group	$P\bar{1}$ (No. 2)	$P\bar{1}$ (No. 2)	$P2_1/n$ (No. 14)
a, Å	7.919(1)	7.835 (3)	22.134(4)
b, Å	10.477(2)	11.387 (4)	8.623(2)
c, Å	10.856(2)	11.447(4)	22.404(5)
α, deg	91.90(1)	83.99(1)	
β, deg	106.09(1)	78.70(1)	95.31(1)
γ, deg	97.71(1)	76.91(1)	
V, Å^3	855.2(3)	973.5(6)	4258(2)
F(000)	472	512	2096
Z	2	2	8
ρ_{calc}, g cm^{-3}	1.842	1.748	1.614
T, K	297	299	298
μ, mm^{-1} (Mo Kα)	1.092	1.072	1.009
abs corr	none	empirical	empirical
transm factor: min/max		0.71/0.93	0.69/0.83
θ_{max}, deg	25	30	25
index ranges	$0 \le h \le 9$	$-11 \le h \le 11$	$-31 \le h \le 31$
	$-12 \le k \le 12$	$-16 \le k \le 16$	$-12 \le k \le 12$
	$-12 \le l \le 12$	$-16 \le l \le 16$	$-31 \le l \le 31$
no. of rflns measd	3044	15 431	43 536
no. of unique rflns	3044	5625	7453
no. of rflns, $F > 4\sigma(F)$	2848	4359	6607
no. of params	242	251	453
no. of restraints	0	2	0
$R(F > 4\sigma(F))^a$	0.029	0.031	0.039
R(all data)^a	0.032	0.049	0.045
R_w(all data)^b	0.074	0.075	0.102
diff Fourier peaks, min/max e Å^{-3}	−0.37/0.64	−0.39/0.52	−1.074 /1.069

^{a} $R = \sum||F_o| - |F_c||/\sum|F_o|$. ^{b} $R_w = [\sum(w(F_o^2 - F_c^2)^2)/\sum(w(F_o^2)^2)]^{1/2}$

[Ru(η^5-C_5H_5)(η(1,2,3)-1-PMe_3-2-buten-1-yl)(PMe_3)]PF_6 (18). A solution of **17** (100 mg, 0.246 mmol) in acetone (5 mL) was treated with PMe_3 (75 μL, 0.738 mmol), and the mixture was stirred for 2 h at room temperature. Upon addition of diethyl ether, a pale yellow precipitate was formed, which was collected on a glass frit, washed with diethyl ether, and dried under vacuum. Yield: 113 mg (95%). Anal. Calcd for $C_{15}H_{29}F_6P_3Ru$: C, 34.82; H, 5.65. Found: C, 34.81; H, 5.70. ^{1}H NMR (δ, acetone-d_6, 20 °C): 4.81 (s, 5H), 4.47 (m, 1H, H^2, J_{HP} = 10.6 Hz, J^{12} = 8.8 Hz, J^{23} = 7.3 Hz, J = 1.8 Hz), 3.51 (m, 1H, H^3, J^{23} = 7.3 Hz, J^{34} = 6.6 Hz, J = 2.4 Hz), 1.97 (d, 9H, J_{HP} = 13.7 Hz), 1.49 (d, 9H, J_{HP} = 8.3 Hz), 1.21 (m, 1H, H^1, J_{HP} = 12.5 Hz, J_{HP} = 12.5 Hz, J^{12} = 8.8 Hz, J = 1.3 Hz), 1.04 (dd, 3H, J^{34} = 6.6 Hz, J = 3.1 Hz). ^{31}P{^{1}H} NMR (δ, acetone-d_6, 20 °C): 30.3, 4.7, −142.7 (s t, PF_6^-, J_{PF} = 707.3 Hz).

Kinetics. The stopped-flow kinetic data were obtained with Hi-Tech SF-40 and Hi-Tech SF-61 instruments. The optical signals at 400 nm (in the case of $PPhMe_2$) and at 355 nm (in the case of P{(2,4,6-OMe)$_3C_6H_2$}$_3$) were monitored. The data were collected as sets of 2.048 and 512 points, respectively, corresponding to 3−4 half-lives.The data were transferred to a DOS/Windows-based personal computer for data analysis. The data all involved pseudo-first-order conditions with the phosphine in large excess over the ruthenium complex. They were fit to one exponential or a sum of two exponentials (in one case, a third exponential was required) using the CURFIT nonlinear least-squares routine of Bevington[36] programmed in QuickBasic or the Hi-Tech IS-2 software suite. The nonlinear least-squares analysis of the dependence of the observed rate constants (k) and amplitudes (A) on phosphine concentration and temperature was performed using the Scientist data analysis package with the points weighted by 1/(k or A)^2. Typically 36 different conditions of phosphine concentration and temperature were utilized, with 3−8 replicate kinetic measurements at each condition.

Most reactions of [Ru(η^5-C_5H_5)(η^4-C_5H_4O)(L)]CF_3SO_3 where L = CH_3CN showed two exponentials and were fit to a rate law for the reversible formation of an intermediate followed by the irreversible formation of the product, as described previously.[3d] This leads to fit parameters (see Scheme 3) for k_{1m}, k_{2m}, and k_{3m} (pathway 1) and k_{1c}, k_{2c}, and k_{3c} (pathway 2). For $PPhMe_2$, a third exponential that was slower and of lower amplitude, and which showed no concentration dependence, was observed. This process was also observed when CH_3CN instead of acetone was the solvent, but its activation parameters were much different. In this case, the two faster processes were treated as for the previously discussed phosphines. For PPh_2Me, the steps were separated further in time so that the reversible first step was studied independently from the product-forming step. In such cases, the concentration dependence is of the form $k_{obs} = k_1$[phosphine] + k_2 and the rate constants are identified with the slope and intercept of the plot of k_{obs} vs [phosphine] as obtained by weighted linear least-squares regression.[36] In the single case of P{(2,4,6-OMe)$_3C_6H_2$}$_3$, two exponentials were observed and the data were fit to the fast preequilibrium formation of one dead end species (identified as the intermediate produced by attack at the metal) and the irreversible formation of a second intermediate (identified as the intermediate produced by attack at C_5H_4O) and then further irreversible formation of the 1,2-disubstituted product. The parameters produced from this treatment are identified as K_m, k_{1c}, and k_{3c}. The assignment of the kinetic processes to mechanistic steps relied on the NMR results and the signs of the amplitudes of the optical changes.

The reaction of [Ru(η^5-C_5H_5)(η^4-C_5H_4O)(L)]CF_3SO_3 where L = pyridine or thiourea and the phosphine PMe_3 and the reaction where L = pyridine or PBu^n_3 showed a single exponential with a positive intercept in the concentration dependence plot. This was attributed to reversible formation of the intermediate formed by attack at the metal and allowed resolution of k_{1m} and k_{2m}. For the reactions with L = pyridine and PPh_2Me as well as for L = thiourea with $PPhMe_2$ and PBu^n_3, a single exponential was observed and attributed to

(36) Bevington, P. R. *Data Reduction and Error Analysis for the Physical Sciences*; McGraw-Hill: New York, 1969.

the irreversible formation of the intermediate formed by attack at C_5H_4O. The rate of the subsequent reaction to produce the 1,2-disubstituted product was measured by NMR methods. For the reaction with L = pyridine and $P\{(2,4,6\text{-}OMe)_3C_6H_2\}_3$ and for the reaction of L = thiourea with PPh_2Me, a similar situation was observed, but the subsequent product formation step could not be studied due to decomposition of the intermediate. The most complex case involves the reaction of PMe_2Ph with the Ru complex in which L = pyridine. This reaction shows two exponentials. One is attributed to the reversible formation of the intermediate formed by attack at the Ru, and the slower one is assigned to the irreversible formation of the intermediate formed by attack at the C_5H_4O ligand. The latter intermediate goes on to the 1,2-disubstituted product at a yet much slower rate, as monitored by ^{1}H NMR spectroscopy. The reaction of **3** with $PMePh_2$ was also monitored by ^{1}H NMR spectroscopy in the temperature range from 0 to 36 °C. The concentration vs time curves were fit to a rate law for the reversible formation of an intermediate followed by the irreversible formation of the product.

The reaction of the η^3 intermediate **7a** with PMe_3 was studied by means of ^{1}H NMR spectroscopy in acetone-d_6 in the temperature range −15 to 0 °C. The rate of disappearance of **7a** and the rate of the appearance of **14a** were followed by integration of the pyridine resonances at 9.2 ppm (**7a**) and 8.7 ppm (**14a**). PMe_3 was in large excess (0.4−1.6 M) over the ruthenium complex (0.04 M) to ensure pseudo-first-order conditions. The linear dependence of the observed pseudo-first-order rate constant on [PMe_3] indicates that the reaction is first order in PMe_3 and second order overall. There was no evidence for an intermediate or a reversible reaction.

The kinetics of the reaction of **2** with pyridine-d_5 in acetone-d_6 as the solvent to give **3** (substitution of CH_3CN by pyridine) were studied by ^{1}H NMR spectroscopy. Pyridine-d_5 was used in large excess (0.4−1.6 M) over the ruthenium complex (0.04 M) to ensure pseudo-first-order conditions. The rate of disappearance of **2**, and the rate of appearance of **3** were followed by integration of the respective C_5H_5 proton resonances. The observed rate constant k_{obs} depended linearly on the concentration of pyridine-d_5, and there was no evidence for an intermediate or reversibility of the reaction. Measurements over the temperature range 3−50 °C yielded the activation parameters.

EHMO Calculations. The extended Hückel molecular orbital calculations were conducted using the program developed by Hoffmann and Lipscomb,[37] as modified by Mealli and Proserpio.[38] The atomic parameters were taken from the CACAO program. All bond lengths and angles of the complexes analyzed were those determined from crystallography or from geometry optimization using a Walsh analysis with initial values taken from known structural data.

Crystallographic Structure Determinations. Crystal, data collection, and refinement parameters are given in Table 3. For **3**, a Philips PW1100 four-circle diffractometer with graphite-monochromated Mo Kα radiation (λ = 0.710 73 Å) and a $\theta-2\theta$ scan capability was used. For **4** CH_3CN and **18**, X-ray data were collected on a Siemens Smart CCD area detector diffractometer (graphite-monochromated Mo Kα radiation, λ = 0.710 73 Å, 0.3° ω-scan frames). Corrections for Lorentz and polarization effects, for crystal decay, and, in the case of **4** CH_3CN and **18,** for absorption were applied. The structures were solved by direct methods.[39] All non-hydrogen atoms were refined anisotropically. Hydrogen atoms were inserted in idealized positions and were refined riding with the atoms to which they were bonded. The structures were refined against F^2.[40]

Acknowledgment. Financial support from the Fonds zur Förderung der wissenschaftlichen Forschung is gratefully acknowledged (Project No. 11182).

Supporting Information Available: Tables S1−S28, listing the kinetic conditions and all of the measured rate constants and amplitude ratios as well as the fit values, and Tables S29−S43, giving atomic coordinates and U_{eq} values, hydrogen coordinates and U_{iso} values, anisotropic temperature factors, complete bond lengths and angles, and least-squares planes for complexes **3**, **4**·CH_3CN, and **18** (47 pages). Ordering information is given on any current masthead page.

OM980701T

(37) (a) Hoffmann, R.; Lipscomb, W. N. *J. Chem. Phys.* **1962**, *36*, 2179. (b) Hoffmann, R.; Lipscomb, W. N. *J. Chem. Phys.* **1962**, *36*, 3489. (c) Hoffmann, R. *J. Chem. Phys.* **1963**, *39*, 1397.

(38) Mealli, C.; Proserpio, D. M. *J. Chem. Educ.* **1990**, *67*, 399.

(39) Sheldrick, G. M. *SHELXS97*: *Program for the Solution of Crystal Structures*, University of Göttingen: Göttingen, Germany, 1997.

(40) Sheldrick, G. M. *SHELXL97*: *Program for Crystal Structure Refinement*; University of Göttingen: Göttingen, Germany, 1997.